

**MODELLING OF DIFFERENT TAPERED  
STRUCTURE OF MULTIMODE INTERFERENCE  
(MMI) COUPLERS.**



**UNIVERSITI TEKNIKAL MALAYSIA MELAKA**

**MODELLING OF DIFFERENT TAPERED  
STRUCTURE OF MULTIMODE INTERFERENCE  
(MMI) COUPLERS.**

**KHAIRUL ANUAR BIN AMINODDIN**



**This report is submitted in partial fulfilment of the requirements  
for the degree of Bachelor of Electronic Engineering with Honours**

**Faculty of Electronic and Computer Engineering  
Universiti Teknikal Malaysia Melaka**

**2022**

## DECLARATION

I declare that this report entitled “Modelling of Different Tapered Structure of Multimode Interference (MMI) Couplers” is the result of my own work except for quotes as cited in the references.



Signature : .....

Author : KHAIRUL ANUAR BIN AMINODDIN  
.....

Date : 11 JANUARY 2022  
.....

## APPROVAL

I hereby declare that I have read this thesis and in my opinion this thesis is sufficient in terms of scope and quality for the award of Bachelor of Electronic Engineering with Honours.



اونيورسيتي تيكنيكل مليسيا ملاك

Signature : .....

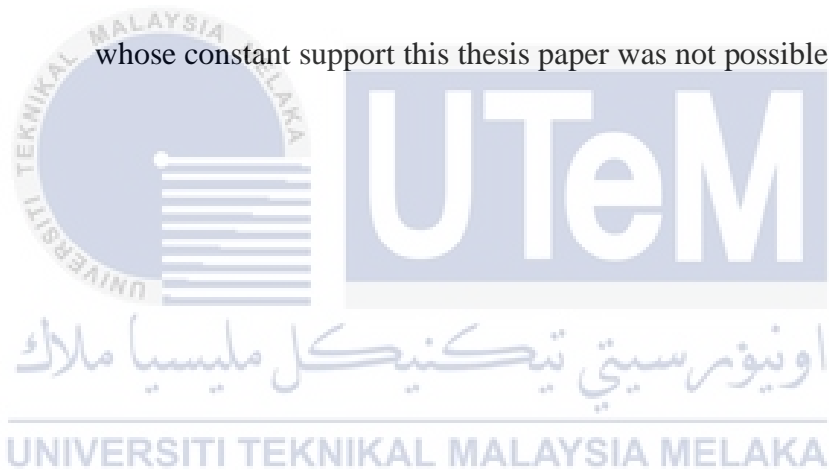
UNIVERSITI TEKNIKAL MALAYSIA MELAKA

Supervisor Name : DR. HANIM BINTI ABDUL RAZAK  
.....

Date : 11 JAN 2022  
.....

## DEDICATION

This work is completely dedicated to my respectful parents and family without whose constant support this thesis paper was not possible.



## ABSTRACT

The demand for a higher bitrate with a high-modulation speed drives the need for developments of photonic integrated circuits (PIC) to overcome the dissipation in the optical channel. The multimode interference (MMI) coupler is one of the structures that can split and combine light for an optical device in PIC. The MMI coupler is commonly used in Mach-Zehnder interferometer (MZI) optical modulator, multiplexing/demultiplexing devices, logic gates, power splitters/couplers, switches, attenuators, and lasers. Multimode interference (MMI) coupler is a compact and sensitive device. Most of the research focuses on reducing the size of MMI by modifying the structure and improving the performance. Recent research suggests that tapering the structure enhances the overall performance of the coupler. This research studies the effect on MMI performance by varying MMI width, MMI length and also tapering the input/output waveguide. The performance was measured by observing the output power ratio and insertion loss (IL). The linear, parabolic, exponential, symmetrical and non-tapered MMI coupler are precisely modelled in OptiBPM designer. Each model is simulated in the OptiBPM 2D simulator to illustrate the optical field propagation and the cut view. Furthermore, the output power and insertion loss are measured in OptiBPM Analyzer. Parabolic tapered with a width of  $26\ \mu\text{m}$  has produced the lowest insertion loss of 0.27 dB. On the other hand, the non-tapered MMI coupler has the worst performance of 1.67 dB. In addition, the symmetrical tapered turn out to be the most compact MMI coupler that can be produced with a minimum length of  $278\ \mu\text{m}$ . A low insertion loss and size compactness demonstrated in this research have portrayed this device's prospect in photonics applications.

## ABSTRAK

Permintaan untuk kadar bit tinggi dengan kelajuan modulasi tinggi mendorong keperluan untuk perkembangan baharu litar bersepadu fotonik (PIC) untuk mengatasi kehilangan isyarat dalam saluran optik. Pengganding interferensi mod pelbagai (MMI) adalah salah satu struktur yang boleh membahagi dan menggabungkan cahaya untuk peranti optik dalam PIC. Pengganding MMI biasanya digunakan dalam modulator optik Mach-Zehnder interferometer (MZI), peranti pemultipleksan /penyahmultipleksan, get logik, pembahagi/peganding kuasa, suis, pelemah dan laser. Pengganding MMI adalah peranti padat dan sensitif. Kebanyakan penyelidikan memberi tumpuan kepada pengurangan saiz MMI dengan mengubah suai struktur dan meningkatkan prestasi. Penyelidikan terdahulu mencadangkan bahawa struktur tirus meningkatkan prestasi keseluruhan pengganding. Penyelidikan ini mengkaji kesan ke atas prestasi MMI dengan mempelbagaikan lebar MMI, panjang MMI dan juga meruncing pandu gelombang input/output melalui pemerhatian nisbah kuasa keluaran dan kehilangan sisipan (IL). Pengganding tidak tirus, linear, parabola, eksponen dan simetri dimodelkan dengan tepat dalam pereka bentuk OptiBPM. Setiap model disimulasikan dalam simulator 2D OptiBPM bagi menggambarkan perambatan medan optik dan paparan potong. Seterusnya, kuasa keluaran dan kehilangan sisipan diukur dalam Penganalisis OptiBPM. Parabola tirus dengan lebar  $26 \mu\text{m}$  telah menghasilkan kehilangan sisipan terendah sebanyak 0.27 dB. Sebaliknya, pengganding MMI tidak tirus memaparkan prestasi terendah iaitu 1.67 dB. Selain itu, tirus simetri menjadi pengganding MMI paling padat yang boleh dihasilkan dengan panjang minimum  $278 \mu\text{m}$ . Kehilangan sisipan yang rendah dan kekompakan saiz yang ditunjukkan dalam penyelidikan ini telah menggambarkan prospek masa hadapan peranti ini dalam aplikasi fotonik.

## ACKNOWLEDGEMENTS

The deepest gratitude to almighty Allah for blessing me with the ability and composure during my research and preparing this thesis within the schedule.

First and foremost, my highest appreciation goes to the Public Service Department (JPA) and Ministry of Communications and Multimedia Malaysia (KKMM) for giving me the opportunity to pursue my studies as an undergraduate student at Universiti Teknikal Malaysia, Melaka (UTeM).

I would like to express my sincere gratitude to my project supervisor, Dr Hanim Binti Abdul Razak. Even in her busyness, she is willing to spend time sharing knowledge and guidance from the very beginning until the completion of my research. I have no hesitation in saying that, without her constant support and valuable advice from time to time, I would probably fail to complete the research appropriately.

I would like to extend my sincere thanks to the course coordinator, Dr Mas Haslinda Binti Mohamad, for assisting me in meeting all the requirements to complete my thesis and technical report.

I would like to express my heartfelt gratitude to my family for their endless support in every way.

Last but not least, during my research, I have received great help from my friends and colleague which I like to express my gratitude and appreciation.



## TABLE OF CONTENTS

<b>Declaration</b>	
<b>Approval</b>	
<b>Dedication</b>	
<b>Abstract</b>	<b>i</b>
<b>Abstrak</b>	<b>ii</b>
<b>Acknowledgements</b>	<b>iii</b>
<b>Table of Contents</b>	<b>iv</b>
<b>List of Figures</b>	<b>vii</b>
<b>List of Tables</b>	<b>x</b>
<b>List of Symbols and Abbreviations</b>	<b>xi</b>
<b>List of Appendices</b>	<b>xiii</b>
<b>CHAPTER 1: INTRODUCTION</b>	<b>1</b>
1.1 Problem Statement.	4
1.2 Project Objective.	4
1.3 Scope of Work.	5
1.4 Project Outcome and Commercialization Potential.	6

1.5	Environmental and Sustainability.	6
1.6	Thesis Outline	7
<b>CHAPTER 2: BACKGROUND STUDY</b>		<b>8</b>
2.1	Principle of Optical Waveguide Propagation.	9
2.2	Waveguide Coupling	13
2.3	Multimode Interference (MMI) Waveguide.	20
2.3.1	Properties and Requirement.	21
2.3.2	Imaging Quality.	21
2.3.3	Balance, Phase and Loses.	22
2.3.4	Reflections Properties.	22
2.4	Tapered Structure of Multimode Interference MMI coupler.	23
2.4.1	Linear Tapered MMI Coupler.	24
2.4.2	Parabolic Tapered MMI Coupler.	29
2.4.3	Exponential Tapered MMI Coupler.	32
2.5	Performance Evaluation Between Tapered Structure.	34
2.6	Design and Analysis Parameter of MMI Coupler.	35
<b>CHAPTER 3: METHODOLOGY</b>		<b>38</b>
3.1	Project Planning and Gantt Chart.	39
3.2	Research Methodology Flowchart.	40
3.3	Detail Description of The Research Methodology Flowchart.	41

3.4	Multimode Interference (MMI) Coupler Design Parameters.	42
3.5	Simulation of Multimode Interference (MMI) Coupler.	46
<b>CHAPTER 4: RESULTS AND DISCUSSION</b>		<b>49</b>
4.1	Non-tapered MMI coupler.	50
4.2	Linear Tapered MMI Coupler.	53
4.3	Parabolic Tapered MMI Coupler.	55
4.4	Exponential Tapered MMI Coupler.	57
4.5	Symmetrical Tapered MMI Coupler.	60
4.6	Input/Output Waveguide Tapered Width.	63
4.7	Performance Evaluation Between Different Tapered Structure.	66
<b>CHAPTER 5: CONCLUSION AND FUTURE WORKS</b>		<b>69</b>
5.1	Conclusion.	69
5.2	Future Works and Recommendations.	71
<b>REFERENCES</b>		<b>72</b>
<b>APPENDIX A.</b>		<b>78</b>
<b>APPENDIX B.</b>		<b>80</b>

## LIST OF FIGURES

Figure 1-1 : The schematic diagram of MMI in MZI Modulator (Chuang et al., 2012).	3
Figure 2-1 : The light refraction and reflection at a medium boundary.	11
Figure 2-2 : The light-wave propagation along a fiber waveguide (Keiser, 2003).	11
Figure 2-3 : The schematic three-layer planar optic waveguide (Huang, 2003).	12
Figure 2-4 : Couplers in an optical fiber communication link (Keiser, 2003).	14
Figure 2-5 : Common design of waveguide coupling.	15
Figure 2-6 : Switched directional coupler (Kogelnik & Schmidt, 1976)	16
Figure 2-7 : Single mode Y-coupler as a splitter.	17
Figure 2-8 : S-Bend waveguide without offset (Okamoto, 2006).	18
Figure 2-9 : $2 \times 2$ double S-bend TMI structure of bending angle A (Sahu, 2011)	18
Figure 2-10 : The schematic diagram of the MMI splitter.	20
Figure 2-11 : The MMI coupler in the MZI modulator.	23
Figure 2-12 : The classification of MMI based on their tapered structure.	24
Figure 2-13 : The linear tapered of 1x2 MMI structure design (Thomson et al., 2010).	25
Figure 2-14 : The proposed design of a 1x4 symmetric power splitter (Shi et al., 2005)	26
Figure 2-15 : The non-tapered tapered design and its simulation result (Chack et al., 2014).	27
Figure 2-16 : The tapered design and its simulation result (Chack et al., 2014).	28

Figure 2-17 : Proposed parabolic tapered structure of a 2x2 symmetric coupler (Sahu, 2013).	30
Figure 2-18 : The 4X4 MMI parabolic tapered (Levy, 1998).	31
Figure 2-19 : Parabolic tapered 1x2 symmetric 3dB power splitter (Wei et al., 2001).	32
Figure 2-20 : Exponential tapered 1x2 symmetric 3dB power splitter (J.-J. Wu, 2008).	33
Figure 3-1 : The three (3) primary tapered structure.	39
Figure 3-2 : Research methodology flowchart.	40
Figure 3-3 : 1x2 MMI power splitter.	43
Figure 3-4 : Linear tapered MMI diagram.	44
Figure 3-5 : Parabolic tapered MMI diagram.	45
Figure 3-6 : Illustration of the four (4) main application in OptiBPM software.	47
Figure 3-7 : The process of designing and simulation in OptiBPM.	47
Figure 4-1: 1x2 MMI Coupler structure in OptiBPM Designer, width=30 $\mu\text{m}$ .	51
Figure 4-2: Optical field propagation of 1x2 MMI Coupler in OptiBPM Analyzer, width=30 $\mu\text{m}$ .	51
Figure 4-3: Non-tapered MMI Coupler output power.	52
Figure 4-4: Non-tapered MMI Coupler insertion loss (IL).	52
Figure 4-5: Linear tapered 1x2 MMI Coupler structure in OptiBPM Designer, width=22 $\mu\text{m}$ .	53
Figure 4-6: Optical field propagation of linear tapered 1x2 MMI Coupler in OptiBPM Analyzer, width=22 $\mu\text{m}$ .	53
Figure 4-7: Linear tapered MMI Coupler output power.	54
Figure 4-8: Linear tapered MMI Coupler insertion loss (IL).	55
Figure 4-9: Parabolic tapered 1x2 MMI Coupler structure in OptiBPM Designer, width=26 $\mu\text{m}$ .	56

Figure 4-10: Optical field propagation of parabolic tapered 1x2 MMI Coupler in OptiBPM Analyzer, width=26 $\mu\text{m}$ .	56
Figure 4-11: Parabolic tapered MMI Coupler output power ratio.	57
Figure 4-12: Parabolic tapered MMI Coupler insertion loss (IL).	57
Figure 4-13: Exponential tapered 1x2 MMI Coupler structure in OptiBPM Designer, width=34 $\mu\text{m}$ .	58
Figure 4-14: Optical field propagation of exponential tapered 1x2 MMI Coupler in OptiBPM Analyzer, width=34 $\mu\text{m}$ .	58
Figure 4-15: Exponential tapered MMI Coupler output power ratio.	59
Figure 4-16: Exponential tapered MMI Coupler insertion loss (IL).	59
Figure 4-17: Symmetrical tapered 1x2 MMI Coupler structure in OptiBPM Designer, width=11 to 22 $\mu\text{m}$ .	61
Figure 4-18: Optical field propagation of symmetrical tapered 1x2 MMI Coupler in OptiBPM Analyzer, width=11 to 22 $\mu\text{m}$ .	61
Figure 4-19: Symmetrical tapered MMI Coupler output power ratio.	62
Figure 4-20: Symmetrical tapered MMI Coupler insertion loss (IL).	62
Figure 4-21: Parabolic tapered 1x2 MMI Coupler structure in OptiBPM Designer, input/output width=2 to 6 $\mu\text{m}$ .	64
Figure 4-22: Optical field propagation of parabolic tapered 1x2 MMI Coupler in OptiBPM Analyzer, input/output width=2 to 6 $\mu\text{m}$ .	64
Figure 4-23: Parabolic tapered MMI Coupler output power ratio.	65
Figure 4-24: Parabolic tapered MMI Coupler insertion loss (IL).	65
Figure 4-25: Insertion loss of different tapered MMI Coupler.	66
Figure 4-26: Length of different tapered MMI Coupler.	67

## LIST OF TABLES

Table 2-1 : Comparison between difference type of optical coupler.	19
Table 2-2 : The simulation result obtained from the design structure.	26
Table 2-3 : The insertion loss (IL) and Extinction ratio (ER)(Chack et al., 2015).	29
Table 2-4 : Linear and Parabolic performance analyzed by (Levy, 1998).	34
Table 2-5 : Parabolic and Exponential performance compared by (J.-J. Wu, 2008).	35
Table 2-6 : Signal to Noise Ratio comparison between output parameters.	37
Table 3-1 : Design parameters of 1x2 MMI Couplers.	45
Table 3-2 : Common simulation parameter for all design.	48
Table 4-1: The design parameter of MMI coupler.	50
Table 4-2: The design parameter of symmetrical tapered MMI coupler	60
Table 4-3: The design parameter of parabolic tapered MMI coupler.	63
Table 4-4: Performance of Different Tapered Structure of MMI Couplers.	68

## LIST OF SYMBOLS AND ABBREVIATIONS

BPM	-	Beam Propagation Method
CAD	-	Computer Aided Design
CMOS	-	Complementary Metal Oxide Semiconductor
dB	-	Decibel
ER	-	Extinction Ratio
FSR	-	Free Spectral Range
GUI	-	Graphical User Interface
IL	-	Insertion Loss
InP	-	Indium Phosphide
LED	-	Light Emitting Diode
LD	-	Laser Diode
MMI	-	Multimode Interference
MUX	-	Multiplexer
MZI	-	Mach-Zehnder Interferometer
PIC	-	Photonic Integrated Circuit
PLC	-	Planar Lightwave Circuit
RIN	-	Relative intensity noise
S/N	-	Signal to Noise Ratio
SNR	-	Signal to Noise Ratio



SOI	-	Silicon-On-Insulator
TE	-	Transverse Electric
TIR	-	Total Internal Reflection
TM	-	Transverse Magnetic
$V\pi L\pi$	-	Modulation Efficiency
WDM	-	Wavelength Division Multiplexing



## LIST OF APPENDICES

<b>Appendix A:</b>	(a)	Project Planning Gantt Chart of PSM 1	78
	(b)	Project Planning Gantt Chart of PSM 2	79
<b>Appendix B:</b>	(a)	Performance of Different Tapered Structure of MMI Coupler.	80



## CHAPTER 1

### INTRODUCTION



اوتنومر سیتی تکنیکا مالسیا ملاک

Human has a fundamental need to interact with one another since ancient times. This requirement sparked interest in developing communication systems that could transmit messages from one location to another. Among the many technologies that people attempted to use, optical communication methods were of particular interest. In the 8th century, the Greeks introduced fire (light) as a warning signal and notification. This was considered one of the earlier applications of an optical communication application. However, visual communication technology was not dynamically developed because of some limitations.

For instance, the transmission rate was restricted to human hand movement, error in human interpretation, line of sight limitation, and weather conditions. In 1970, researchers at Corning demonstrated the feasibility of manufacturing a glass fiber with

an optical power loss low enough for a practical transmission connection, which marked the beginning of the optical fiber communications revolution (Hinch & Miller, 1998). Telecommunication companies around the world have massively increased the ability of fiber lines to meet the ever-increasing demand for high-bandwidth networks ranging from home-based PC users to large corporations and research organizations. This was achieved by the transmitting speed of information carried by each wavelength and adding more separate signal carrying wavelengths on individual fibers.

Nevertheless, electrical technology is also used in the switching parts of fiber optic transmission networks. This could result in several issues, including high power consumption, electromagnetic noise, slow circuit speeds, and restricted bandwidth (Bailey & Wright, 2003).

As the demand for higher bitrate internet with a high-modulation speed (100Gb/s and beyond), new photonic integrated circuits (PIC) are being developed that need more optical level power to overcome the optical channel's losses. To solve this problem, a powerful laser with a hundred milliwatts of power can be used. However, nonlinear effects can occur, resulting in a significant reduction in device output and a higher cost when compared to a standard laser. A power splitter and combiner waveguide system are a better option (Samoi et al., 2020).

The wavelength division multiplexing (WDM) is commonly employed in the optical fiber transmission system to handle large data transferred simultaneously. Furthermore, these systems consist of the transmitter and receiver to carry all the signals. Inside the transmitter of the WDM system, an array of lasers will generate the optical carriers. These optical data is then modulated by an external modulator such

as the Mach-Zehnder interferometer (MZI) optical modulator structure (Chuang et al., 2012).

The multimode interference (MMI) coupler is one of the structures that can split and combines light for an optical device in photonic light-wave circuits (PLC). The MMI coupler is commonly used in Mach-Zehnder interferometer (MZI) optical modulator devices as shown in Figure 1-1.

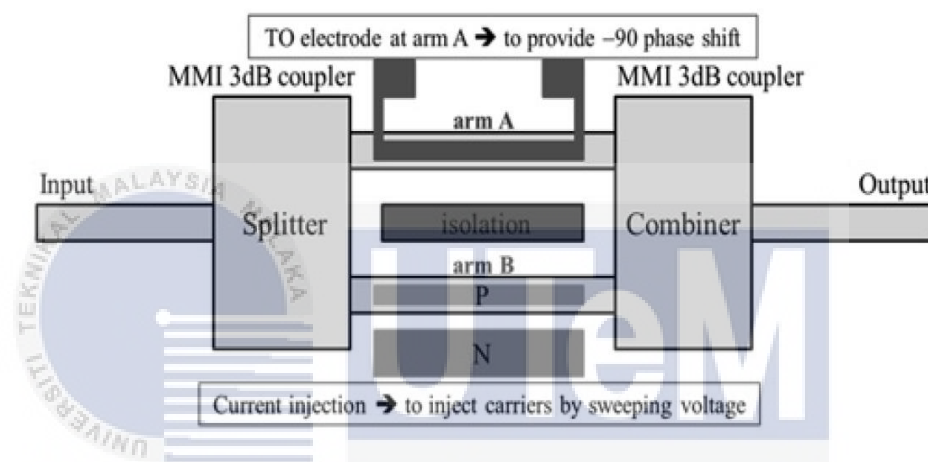


**Figure 1-1 : The schematic diagram of MMI in MZI Modulator (Chuang et al., 2012).**

The structure of MMI is divided into two (2) categories, tapered and non-tapered. Previous research suggests that the tapered structure significantly enhances the overall performance of the coupler. The MZI optical modulator consists of the splitter (input MMI), the phase modulator and the combiner (output MMI). The phase modulator is the electrical part of the MZI optical modulator. The performance of modelled MMI structure will be analyzed and observed using beam propagation method software, OptiBPM.

## 1.1 Problem Statement.

The expanding demand for higher bitrate internet with a high-modulation speed (100Gb/s and beyond) drives new developments of photonic integrated circuits (PIC) that need a higher optical level power to overcome the losses of the optical channel. A powerful laser with 100mW of power can be used. However, nonlinear effects can occur for a microchip circuit, resulting in a significant reduction in device output and a higher cost when compared to a standard laser. A power splitter and combiner waveguide system are a better option (Samoi et al., 2020). Multimode interference (MMI) devices are very significant module in complex photonic integrated circuits (PIC) such as Mach-Zehnder Interferometer (MZI), multiplexing/demultiplexing devices, logic gates, power splitters/couplers, switches, attenuators, and lasers. A recent study shows that tapering the structure of MMI produces a significant impact on enhancing splitting and combining performance (Besse et al., 1994; Pachnicke et al., 2012; Shi et al., 2007). Hence, this research will model and analyze the performance of the different tapered structure of MMI coupler. The data and simulations result can be used as a reference in an optical industry and the future development of MMI coupler. Modelling in simulation software would significantly optimize the development time frame, reduce the cost of laboratory testing and fabrications.

## 1.2 Project Objective.

The main objective of this research is to model and analyze the effect of tapering the waveguide structure of Multimode Interference (MMI) coupler. In detail, the research objective is as follow.

1. To design and model a different tapered structure of MMI coupler.
2. To simulate the design using OptiBPM software.
3. To analyze and compare the performance of different tapered structure of MMI coupler.

### 1.3 Scope of Work.

The scope of the project specifies the focus and the limitations on achieving the project objective. This project is limited to computational analysis, using the simulation tool which utilized the Beam Propagation Method (BPM). In several points, at the earlier stage of conceptual designing, some mathematical formulation is needed to obtain an accurate dimension of the MMI coupler. The scope of the project is covered by five (5) tasks and parameters.

1. Modelling and simulation of different tapered structure of MMI coupler in OptiBPM software.
2. The design structure is linear tapered, parabolic tapered and exponential tapered.
3. The design parameter focuses on MMI region width, MMI region length, waveguide width and waveguide length.
4. All design in this project employs a waveguide refractive index of 3.45, a cladding refractive index of 1.0 and a wavelength of 1550nm.
5. The result and performance are analyzed in terms of insertion loss (IL).

#### **1.4 Project Outcome and Commercialization Potential.**

1. Produce a modelling of different tapered MMI coupler and demonstrate each design's performance in terms of structure compactness and losses.
2. Promoting the potential of MMI coupler in optical technology through this research paper would significantly increase MMI Coupler's usage in multiple applications such as multiplexing/demultiplexing devices, logic gates, power splitters/couplers, switches, attenuators, and lasers.

#### **1.5 Environmental and Sustainability.**

1. Modelling in simulation software would significantly optimize the development time frame, reduce the cost of laboratory testing and fabrications.
2. A low loss MMI coupler can contribute to good energy consumption for the overall optical modulator system.
3. Compared to a linear structure, this tapered structure is less in size, less in the volume of material and insensitivity to fabrication tolerances. All these parameters are significantly crucial in precision engineering.
4. A better performance component will increase the stability and life span of the system.



## 1.6 Thesis Outline

Chapter 1 briefly introduces MMI coupler in optical communication, problem statement, project's objectives, the scope of work, project outcome, and project impact on the environment and sustainability.

Chapter 2 covered the project's background study, including the principle of optical waveguide propagation, waveguide coupling, Multimode Interference MMI coupler, different tapered of MMI coupler, and performance evaluation parameters.

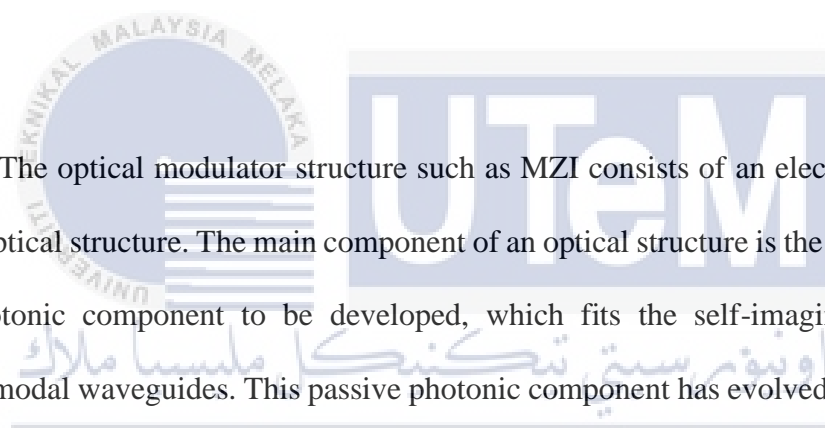
Chapter 3 focuses on the methodology of this project, which includes the research methodology flowchart, Multimode Interference MMI coupler design parameters, simulation procedure and analyzer.

Chapter 4 consists of the project simulation result, the analysis, and discussions.

Chapter 5 summarize all the completed works and discusses some recommendations for future research.

## CHAPTER 2

### BACKGROUND STUDY



The optical modulator structure such as MZI consists of an electrical structure and optical structure. The main component of an optical structure is the MMI Coupler, a photonic component to be developed, which fits the self-imaging concept of multimodal waveguides. This passive photonic component has evolved due to interest in its effects in integrated optics and its advantages. This component specifically, provides higher fabrication tolerances and polarization independent performance, all of which are very useful (Besse et al., 1994). Although this passive component small and compact in size the former can be used as multiplexing/demultiplexing devices (Shi et al., 2007), logic gates (Li et al., 2005), power splitters/couplers (Soldano & Pennings, 1995), switches (Wang et al., 2006), attenuators (Jiang et al., 2005), and lasers (Hamamoto et al., 2001). For MMI coupler the structure is generally referred to as NxM, where N is referred to as input and M is the output.

Recent research shows that MMI performs better than Y-coupler, novel star coupler, and directional coupler. The analysis has been made in terms of the extinction

ratio where MMI is approximately  $> 32\text{dB}$  whilst Y-coupler and novel star only  $10\text{dB}$  and  $14\text{dB}$  respectively (Thomson et al., 2010). Comparing to Y-coupler, MMI has better modulation efficiency and insertion loss of  $2.53\%$  and  $17\%$  respectively (Razak et al., 2015). Another interesting fact about MMI, the splitting ratio is relatively insensitive to device temperature changes, and optical throughput is only marginally affected (Thomson et al., 2010). The loss caused by the modal mismatch between the MMI region, and the input and output waveguides are one downside of this structure. Some theoretical studies show that tapering input and output waveguides can significantly reduce the loss (Halir, Ortega-Monux, et al., 2009).

## 2.1 Principle of Optical Waveguide Propagation.

Optical parameter principles of a material are the refractive index, wherein in free space, a light wave travels at a speed  $3 \times 10^8 \text{m/s}$ . The speed of light in free space

( $c$ ) is related to the frequency ( $f$ ), and the wavelength ( $\lambda$ ) with the ratio is given by,

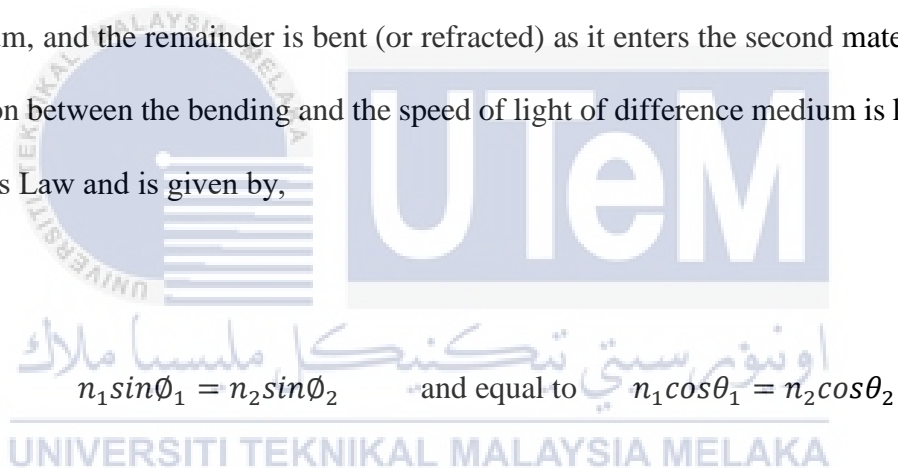
$$c = f\lambda$$

When the light enters the non-conducting medium which characteristic is less than ( $c$ ) the ratio is given by,

$$n = \frac{c}{v}$$

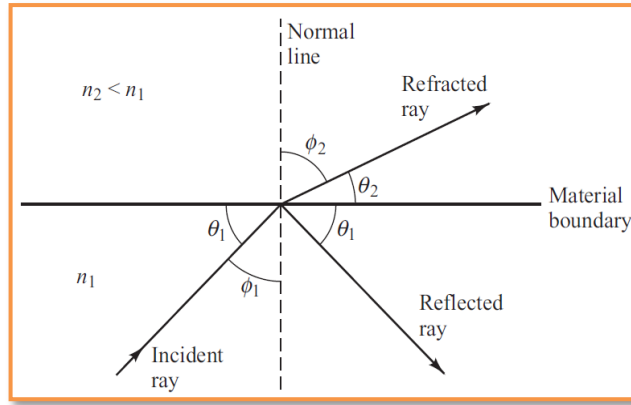
Where,  $n$  is the material refractive index,  $c$  is the speed of light in vacuum and  $v$  is the speed of light in the medium (Keiser, 2003). This ratio is called the index of refractive. Optical waveguides or optical fibers is developed from two primary structure, a core that confined lights, and a cladding surrounding the core. The light beam is confined in the core of the waveguide when the refractive index of the core  $n_1$  is higher than that of the cladding  $n_2$ . This condition is called total internal refraction (TIR).

The concepts of reflection and refraction happen when a light ray encounters a boundary separating two different media, part of the ray is reflected into the first medium, and the remainder is bent (or refracted) as it enters the second material. The relation between the bending and the speed of light of difference medium is known as Snell's Law and is given by,



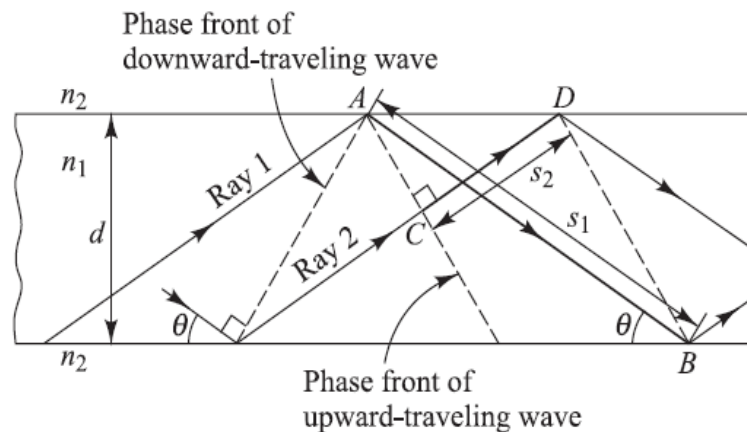
$$n_1 \sin \phi_1 = n_2 \sin \phi_2 \quad \text{and equal to} \quad n_1 \cos \theta_1 = n_2 \cos \theta_2$$

Figure 2-1 displays the light refraction and reflection at a medium boundary. As the angle of incidence  $\phi_1$  in denser material becomes larger, the refracted angle  $\phi_2$  approaches  $90^\circ$  the light rays become totally internally reflected (TIR) (Okamoto, 2006).



**Figure 2-1 : The light refraction and reflection at a medium boundary.**

The critical angle in which the total internal reflection (TIR) occurs is given by equation  $\theta_c = \sin^{-1}(n_2/n_1)$ . The situation wherein refractive index of material  $n_2$  is lesser than  $n_1$  ( $n_2 \leq n_1$ ). When the interference effect caused by the phase of the plane wave associated with the ray is considered, only waves with discrete angles higher than or equal to  $\theta_c$  can propagate along the fiber. The geometry of waves reflecting at material surfaces is shown in Figure 2-2 . Looking at ray 1 and ray 2, that are both related with the same wave. At an angle of  $\theta < \theta_c = 90^\circ - \theta_c$ , the rays are incident with the material interface.



**Figure 2-2 : The light-wave propagation along a fiber waveguide (Keiser, 2003).**

The phase of a wave changes not only as it travels, but also when it is reflected off a dielectric medium. In the dielectric slab waveguide, only waves with angles  $\theta$  that satisfy the requirement in equation below will propagate (Keiser, 2003).

$$\tan \left( \frac{\pi n_1 d \sin \theta}{\lambda} - \frac{\pi m}{2} \right) = \left[ \frac{\sqrt{n_1^2 \cos^2 \theta - n_2^2}}{n_1 \sin \theta} \right]$$

A planar waveguide form by large planar core with thickness related to the wavelength and a higher reflective index than the cladding. Figure 2-3 shows the schematic three-layer planar optic waveguide. The light travels in the z-axis, is contained in the x-axis within the central core region and has no fluctuation in the y-axis (Huang, 2003).

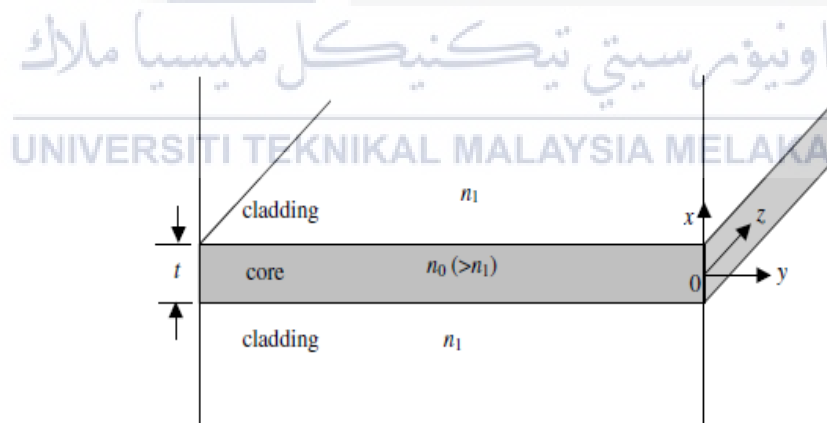


**Figure 2-3 : The schematic three-layer planar optic waveguide (Huang, 2003).**

Furthermore, the fields are independent to y-axis. The TE and TM mode are stated as equation given by,

$$\text{TE : } \frac{d^2 e_y}{dx^2} + k^2 \left( n_{yy}^2 - n_e^2 - \frac{n_{xy}^4}{n_{xx}^2 - n_e^2} \right) e_y = 0$$

And,

$$\text{TM : } \frac{d^2 h_y}{dx^2} + p \frac{dh_y}{dx} + k^2 \frac{n_{zz}^2}{n_{xx}^2} \left( n_{xx}^2 - n_h^2 - \frac{n_{xy}^4}{n_{yy}^2 - n_e^2} \right) h_y = 0$$

Where;

$$p(x) = \frac{-2}{n_{zz}} \frac{dn_{zz}}{dx}$$

UNIVERSITI TEKNIKAL MALAYSIA MELAKA

## 2.2 Waveguide Coupling

Coupling can be conceived of as the transmission of power from one medium or circuit to another in terms of electromagnetics. Coupling between media that are designed to work in isolation is undesirable and can result in performance degradation as well as negative consequences on electrical circuits. Couplers are essential components in optical communication systems because they allow power to be transferred, routed, split, and combined at any point in the system. Fiber couplers that are ideal should diffuse light evenly throughout the branch's fibers. There should be

no loss, and they should be completely insensitive to light distribution between fiber modes as well as the state of polarization of light (Shaim & Khan, 2011). Optical data transmission requires the efficient transfer of power from fibers to photonic integrated circuits, which necessitates the development of efficient, compact, and wideband optical couplers (Emara, 2021).

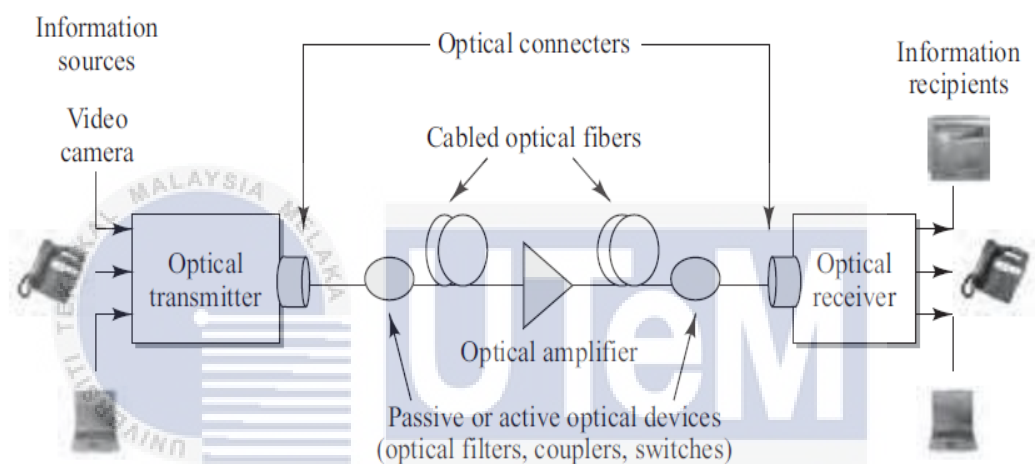


**Figure 2-4 : Couplers in an optical fiber communication link (Keiser, 2003).**

Couplers are mostly used in optical and microwave systems as shown in Figure 2-4. In an optical system, a coupler is used as power combiners and power dividers (B. Wu et al., 2019), integral components in variable optical attenuators (Ke et al., 2006), switches between waveguide through phase mismatch application (Kogelnik & Schmidt, 1976), and optical switching and demultiplexing (Saleh & Teich, 2019). For the microwave system, the principles design of active micro ring resonator dispersive structures at millimeter-waves is based on a directional coupler.



Depending on the application, efficiency, footprint, and bandwidth requirements, different couplers are required. To meet performance requirements, couplers come in a variety of different forms of technology-based devices. One popular approach for transferring power via the fiber core cross-section is to butt join the fibers or use imaging optics between the fibers (core interaction type). Another technology converts directed core modes to cladding and refracted modes on the fiber surface, normal to its axis, allowing the power sharing mechanism to work (Shaim & Khan, 2011).

Couplers have various configurations, and the most used are directional coupler, three-port T or Y junction, multimode interference, and S-bend coupler. Couplers have various configurations, and the most used are directional coupler, three-port T or Y junction, multimode interference, and S-bend coupler. In term of performance, these couplers have their advantages over one and another. Figure 2-5 displays the various design of waveguide coupling.

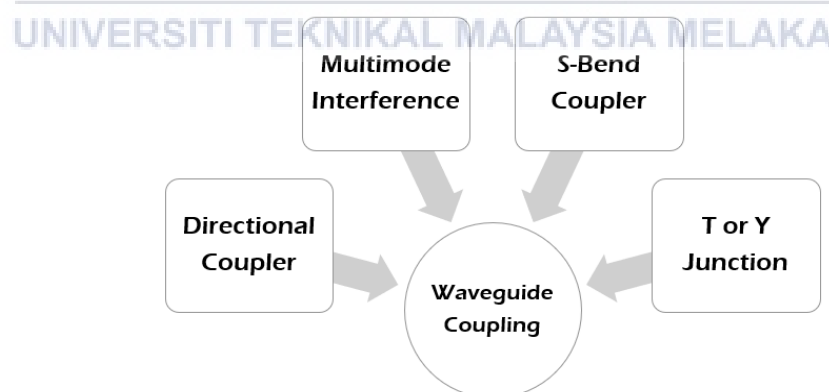


**Figure 2-5 : Common design of waveguide coupling.**

A directional coupler is formed by two parallel strip waveguides. The characteristic is determined by the interaction length, the coupling coefficient, the corresponding conversion length, and the mismatch between the propagation constant (Kogelnik & Schmidt, 1976). Figure 2-6 displays the switched directional coupler. The complete crossover occurs when the guide is phase match, and the interaction length is at an exact odd multiple of coupling length. The interaction length is very important parameter, if it not made exactly equal to the coupling length then the crossover is not complete and will result crosstalk.

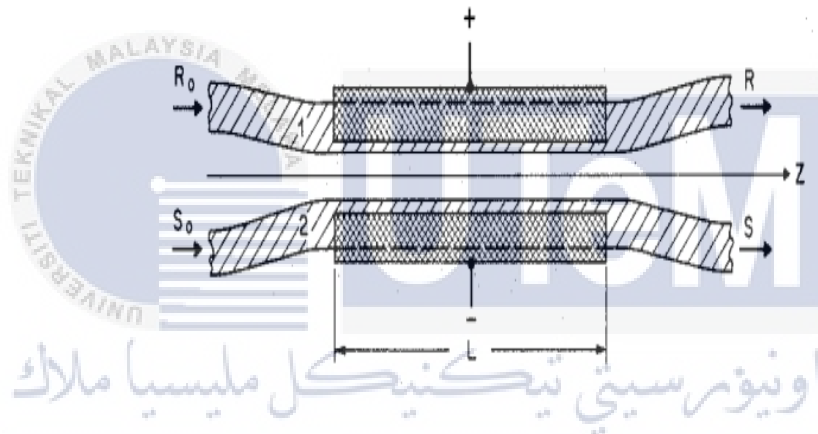


**Figure 2-6 : Switched directional coupler (Kogelnik & Schmidt, 1976)**

Y-couplers is also known as 3 dB couplers, can split the light equally. As shown in Figure 2-7, the light entering Port 1 will be split equally between Ports 2 and 3 with almost no loss. They are highly efficient at splitting light with minor loss. Y-couplers are easy to build in planar waveguide systems compared to construct in fiber optics. Y-couplers are manufactured on the same substrate as other devices, and it is very seldom to build as separate planar devices. Y-couplers is used extensively in complex planar devices compared to fiber optic cable because of significant loss experienced (Al-Azzawi, 2017). The important parameter in designing this type of couplers is the

separation angle between junctions. As illustrated in the Figure 2-7, the Y connection can be separated into three portions. The distance between the two branches in the branching section decreases toward the section's end, where the branches connect. Following the branching portion, a tapered portion seamlessly turns the wide guide into a single-mode straight-guide portion. It is worth mentioning that the radiation mode at the junction results in a necessary optical loss. The single-mode Y junction is viewed as a four-port device when the radiation mode is taken into consideration, and the required power conservation is met at the junction (Izutsu et al., 1982).

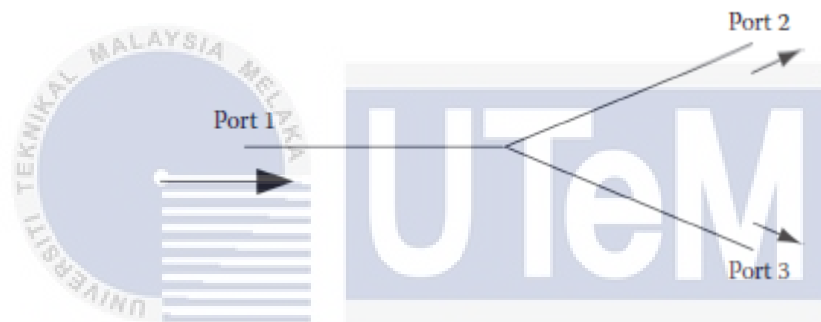


**Figure 2-7 : Single mode Y-coupler as a splitter.**

UNIVERSITI TEKNIKAL MALAYSIA MELAKA

As shown in the Figure 2-8, the S-bend shape waveguide connects two parallel waveguides separated by the distance  $S_b$ . This type of design primarily used as input or output waveguides for couplers and waveguide path transformers in various circuits. Basically, there are two types of S-bend waveguides, first, a fixed radius of curvature  $R$  and second, S-bend waveguide with the functional shape of  $y = ax + b\sin(cz)$  in which radius of curvature varies continuously. The S-bends waveguide's design structure is believed to lower the structure's lengths, but this structure will eventually add excess loss, also known as the structure's insertion loss (Okamoto).

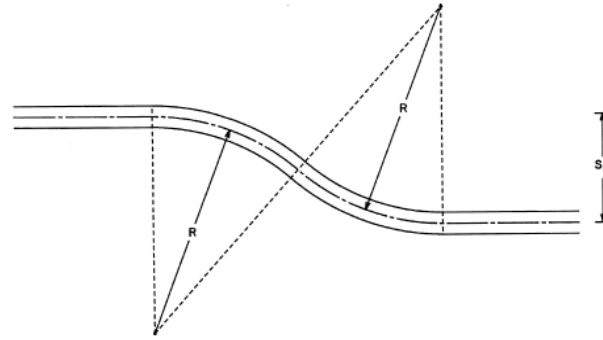


**Figure 2-8 : S-Bend waveguide without offset (Okamoto, 2006).**

Another researcher (Sahu, 2011) proposed a double S-bend TMI coupler. The intention is to study the effect of tapered structure on fabrication tolerance and its power imbalance. With the double S-bend structure in the design, the longitudinal length of  $2 \times 2$  TMI coupler can be reduce. The design parameter is focusing on the height [ $H = S \sin A$ ], longitudinal length [ $L_c/2 = S \cos A$ ] where  $S$  is the S-bend length of TMI region and,  $A$  angle at  $Z$ -direction. Figure 2-9 displays the  $2 \times 2$  double S-bend TMI structure of bending angle  $A$ .

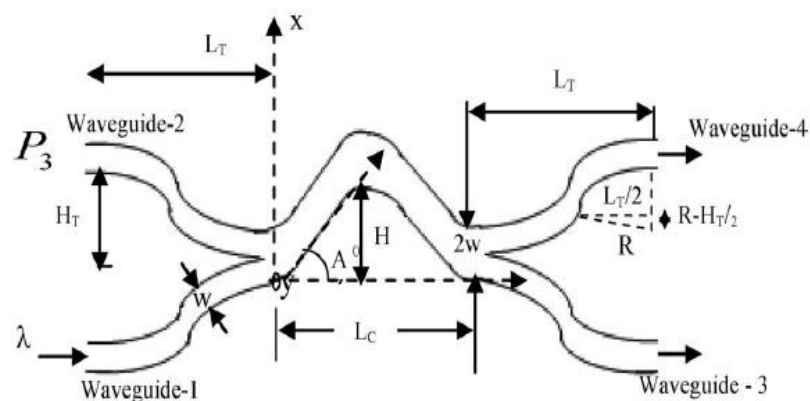


**Figure 2-9 :  $2 \times 2$  double S-bend TMI structure of bending angle  $A$  (Sahu, 2011)**

The simulation result has shown that the longitudinal beat length ( $L\pi$ ) of the proposed TMI coupler with  $\Delta n=5\%$  and bending angle  $\sim 32^\circ$  is reduced by  $\sim 15\%$  of the beat length of a conventional TMI coupler. The increase of power imbalance with  $\pm \delta w$  values are approximately identical for the design structure and the conventional TMI structure reported by another researcher. Table 2-1 displays the comparison between coupler design and performance presented by previous researcher. From the data shown, MMI coupler is significantly produces the best performance among all. It can be concluded that MMI gives a stable performance in splitting and combining of optical source. In the next section of this paper, the details on MMI coupler were studied and analyzed.

**Table 2-1 : Comparison between difference type of optical coupler.**

Waveguide Coupler	Researcher	ER (dB)	IL (dB)	Modulation Efficiency
MMI	(Cherchi et al., 2016)	>15	<1.5	n/a
MMI	(Halir, Ortega-Moñux, et al., 2009)	>22	<1	n/a
MMI	(Thomson et al,2010)	> 32	n/a	n/a
Directional coupler	(Quan et al., 2008)	5-10	22-24	n/a
Y-splitter	(Thomson et al,2010)	10	n/a	n/a
Y-Splitter	(Liow et al., 2010)	5.1	n/a	2.56 V.cm
Y-Splitter	(Liu et al., 2004)	>16	15.3	8 V.cm
Star Coupler	(Marris-Morini et al., 2008)	14	5	n/a
Star Coupler	(Thomson et al,2010)	14	n/a	n/a

### 2.3 Multimode Interference (MMI) Waveguide.

The MMI central structure acts as a waveguide for light propagation from input to output. The MMI couplers can be utilized to split and combine the light signal in association with the MZI optical modulator design. Figure 2-10 shows the image of the basic MMI splitter design. This layout of the splitter allows an efficient optical signal transfer across the device in a shorter device length. The width and length of the MMI structure are very crucial in modelling the device.

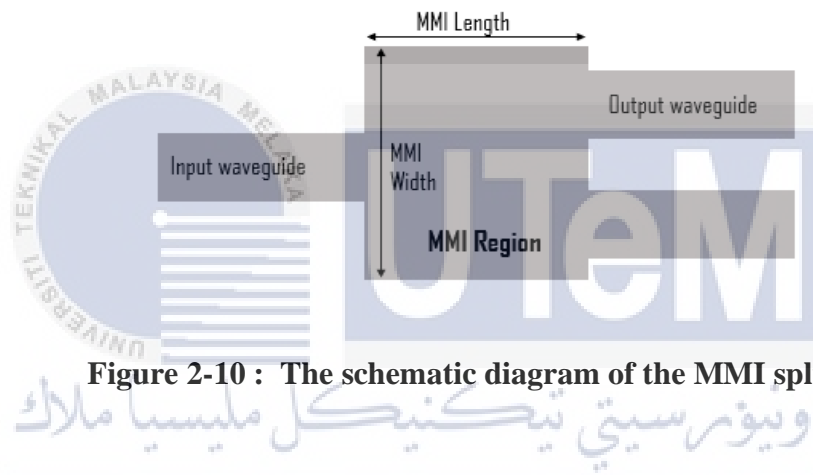


**Figure 2-10 : The schematic diagram of the MMI splitter.**

Coupling of signals in MMI couplers is fundamentally different from device coupling with a directional waveguide. The MMI couplers work based on self-imaging effects in two-dimensional spaces. Self-imaging is a phenomenon of multimode waveguides where an input field profile is repeated at periodic intervals in single or multiple images along the propagation path of the guide (Soldano & Pennings, 1995). The energy transfer is not the same as with a directional coupler. Light is distributed into a wide region with reflective boundaries in the MMI coupler. The beam emitted into the regions will go through diffractions and interferences, resulting in the creation of many focal planes. After a beat duration,  $L$  of the MMI field, the input image will

be reformatted once more. The MMI coupler's output waveguides are used to retrieve signals from the MMI's input (Fujisawa & Koshiba, 2006).

In many ways, MMI devices vary from other routing and coupling devices. To explain how self-imaging influences the design and actions of MMI devices, a few crucial aspects have to be indicated (Soldano & Pennings, 1995).

### 2.3.1 Properties and Requirement.

The location and shape of the input fields have no effect on the general interference mechanism. Careful placement of the access waveguides will improve the efficiency of MMI devices based on general interference. Restricted (paired and symmetric) interference mechanisms require a symmetric input field that is well-located. Due to lower image resolution, general interference mechanisms in weakly guiding structures can suffer higher losses than paired interference.

### 2.3.2 Imaging Quality.

The imaging efficiency of a multimode waveguide refers to how well the input field is replicated at the end (Soldano & Pennings, 1995). The line-spread function can be used to determine the imaging efficiency of a multimode waveguide. A narrow-peak and low-ripple LSF characterizes a high-resolution and good-contrast imaging device. Low insertion loss and low crosstalk are indicated by a narrow-peak and low-ripple LSF, respectively. In the design of an MMI coupler, the imaging resolution is a useful parameter. The image field of the multimode waveguide must be as narrow as the input fields launched from the access waveguides.

### 2.3.3 Balance, Phase and Loses.

Due to the efficient imaging of the MMI section's input onto the output, MMI effects can generate low-loss devices. Furthermore, increased guide separation prevents coupling between the access guides, resulting in a rapid onset of coupling in the MMI segment. This eliminates the need for additional, difficult-to-control power exchange in the access guides, as well as the resulting radiation losses, which is a common problem in directional couplers. Balancing is more critical than insertion loss in many applications. The 3-dB coupler output balances would affect the local oscillator RIN noise suppression (coherent detection method). Furthermore, the 3-dB coupler application in the MZI modulator would directly impact the extinction ratio and crosstalk.

### 2.3.4 Reflections Properties.

Reflections are extremely sensitive in several applications, including lasers and coherent detection techniques. Reflections in MMI devices can originate between the output guides at the end of the MMI-section. There are two distinctive types of reflection mechanisms. First, a simultaneous emerging self-image would generate the internal resonance mechanism. Second, the reflection occurs for the MMI splitter that operates backwards as an optical combiner. For optimal combining, the inputs must be balanced in phase and amplitude. In contrast, the power would be lower at the guide output and higher at the reflecting end for the phase difference of 180 degrees.

In recent years, various tapered MMI structures have been developed and analyzed to improve the performance and size such as linear tapered (Thomson et al.,



2010), parabolic tapered (Sahu, 2013), exponential tapered (J.-J. Wu, 2008), elliptical, and co-sinusoidal tapered (Levy, 1998). Tapered MMI structure can produce a better MZI modulator device reduce the bending loss and increase the optical signal propagation. Important parameters to be considered in modeling difference tapered MMI couplers such as extinction ratio (ER), insertion loss (IL), modulation efficiency (VL), length, and width (Razak et al., 2015). Figure 2-11 shows the MMI coupler in the MZI modulator.

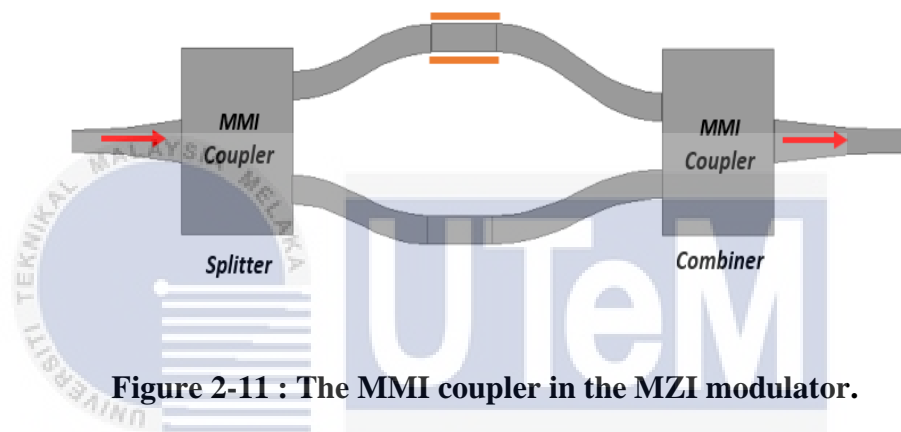


**Figure 2-11 : The MMI coupler in the MZI modulator.**

#### 2.4 Tapered Structure of Multimode Interference MMI coupler.

The resultant from a recent research paper, as mentioned above, has shown that tapering at the input and output waveguide of MMI gives a significant improvement in increasing the extinction ratio, reduce loss and minimize the size of the optical device. By Referring to previous research, the tapered structure can be classified into three (3) difference group such as linear tapered (Thomson et al., 2010), parabolic tapered (Sahu, 2013), exponential tapered (Wu, 2008). Figure 2-12 shows the classification of MMI based on their tapered type. This research will be focusing on modelling the difference type of tapered structure of multimode interference (MMI).

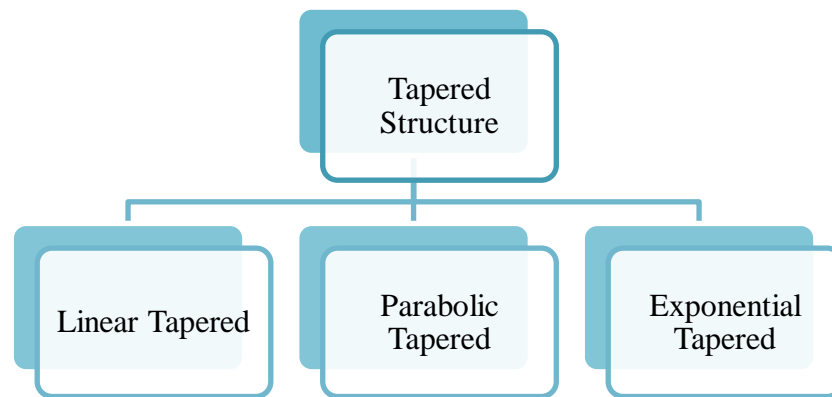


**Figure 2-12 : The classification of MMI based on their tapered structure.**

This research will utilize the beam propagation method BPM software in modelling and analyzing the performance of each design to achieve better power gain and decrease losses.

#### 2.4.1 Linear Tapered MMI Coupler.

A linear tapered structure has been proposed by (Thomson et al., 2010) to improve the performance of multimode interference MMI coupler in Mach-Zehnder Interferometer (MZI) optical modulator. The design proposed is based on the structure of a 1x2 symmetric power splitter, as shown in Figure 2-13. The design intention is to operate at a wavelength of  $1.55\mu\text{m}$  and was built upon SOI strip waveguides. The researcher uses a waveguide height, of 220nm, and an input/output waveguide width, of 400nm. To ensure that the output waveguides are sufficiently separated and compact, the width of the MMI region,  $W_e$ , was chosen to be  $6\mu\text{m}$ . This will avoid evanescent coupling from one to the other. Figure 2-13 shows the linear tapered of 1x2 MMI structure design by the researcher.

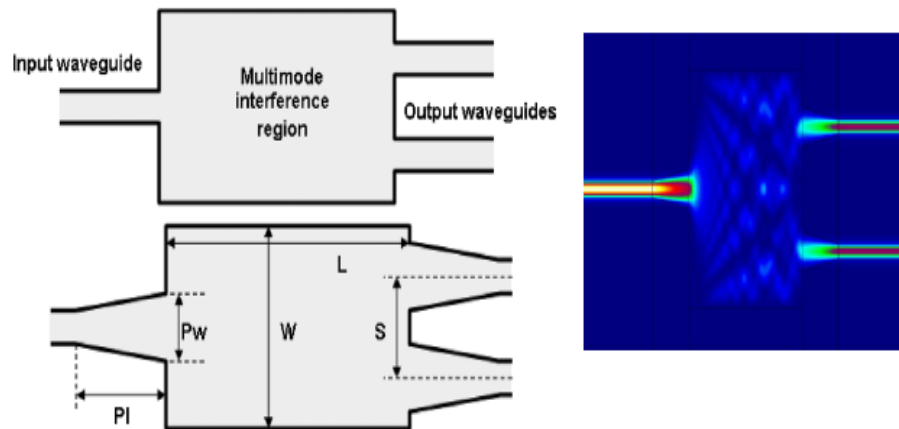


**Figure 2-13 : The linear tapered of 1x2 MMI structure design (Thomson et al., 2010).**

By referring to the fundamentals of self-imaging where  $L$  increasing quadratically with  $W$  and a symmetric two-fold self-image length. The length of MMI region is carefully designed based on the given equation.

$$L_{MMI} = \frac{3\pi}{8(\beta_0 + \beta_1)}$$

Where  $\beta_0$  and  $\beta_1$  are the propagation constant of principle and first order nodes in MMI region. Linear tapered where use at both, input, and output. From the simulation result, the researcher summarizes that the loss then subsequently reduces with increasing taper width. This result highlights that sub-1-dB losses are achieved as the port width is increased above 1000 nm, close to the predicted value of 900 nm and large static extinction ratios achieved ( $\leq 32$ dB), but the MZI extinction ratio is insensitive mainly to MMI port width.

A linear tapered 1X4 MMI structure was proposed by (Shi et al., 2005) to improve the performance of multimode interference MMI coupler in Mach-Zehnder

Interferometer (MZI) optical modulator. The design proposed is based on the structure of a 1x4 symmetric power splitter, as shown in Figure 2-14. The researcher uses an input waveguide width, of  $4\mu\text{m}$  and the MMI region width of  $60\mu\text{m}$ . The length of MMI region is set at  $2089\mu\text{m}$ . The output waveguide is set at located at  $x = 23.3\mu\text{m}$ ,  $7.9\mu\text{m}$ ,  $-7.9\mu\text{m}$  and  $-23.3\mu\text{m}$ .

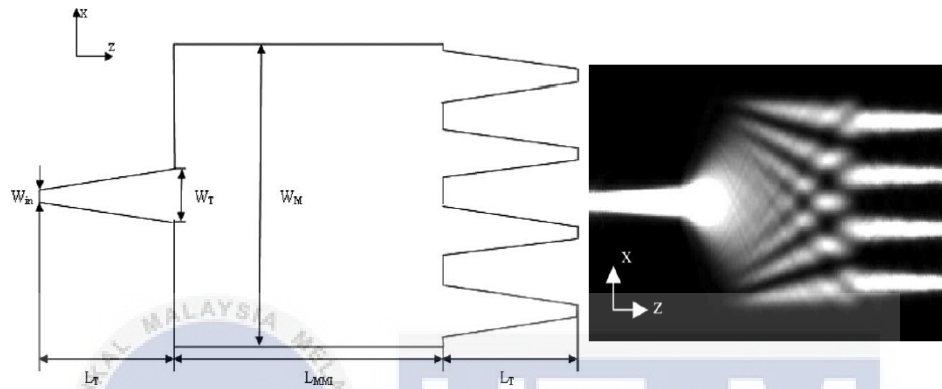


**Figure 2-14 : The proposed design of a 1x4 symmetric power splitter (Shi et al., 2005)**

From the simulation result, the researcher summarizes that the insertion loss (IL) is inversely proportional to the tapered width. Furthermore, the non-uniformity of the i/o power is also stated and verify that tapering significantly reduce loss. Table 2-2 shows the simulation result obtained from the design structure.

**Table 2-2 : The simulation result obtained from the design structure.**

	Non-Tapered MMI	Linear Tapered MMI
Insertion Loss (dB)	1.2127 dB	0.076 dB
Non-uniformity (dB)	0.5509 dB	0.068 dB

Another researcher shows interest in analyzing the effects of manipulating the separation distances ( $s$ ) and arm angle ( $\alpha$ ) on non-tapered and tapered MMI structures (Chack et al., 2014). The Self-imaging fundamental has influenced the design characteristic of MMI devices. The researcher also highlights the tapered MMI structure used is the combination of the series of prism sections. Figure 2-15 shows the non-tapered tapered design and its simulation result.

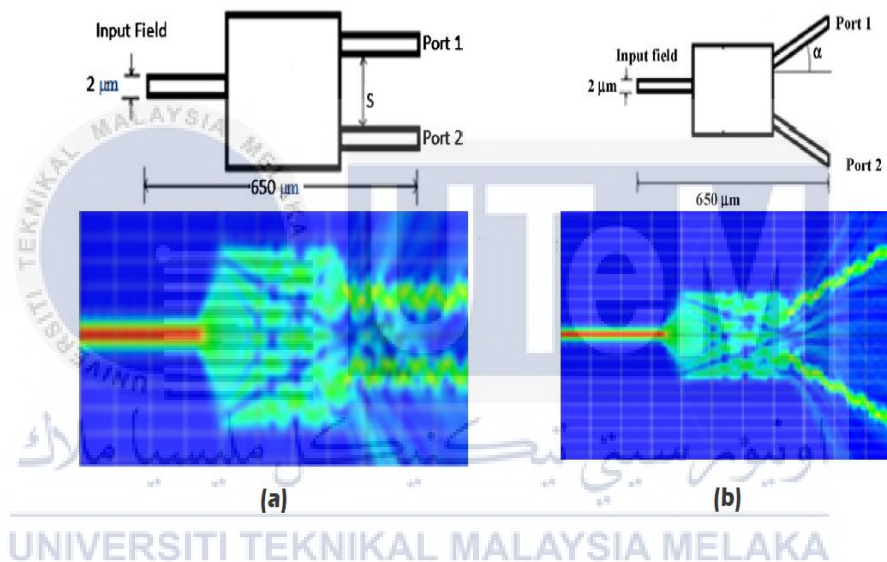


**Figure 2-15 : The non-tapered tapered design and its simulation result (Chack et al., 2014).**

All the structure uses a standardize MMI region length at  $650\mu\text{m}$ . At the same time, the separation distance of the output waveguide is varied between  $4\mu\text{m}$  to  $12\mu\text{m}$ . The output waveguide arm is varied from  $0^\circ$  to  $6^\circ$ . Figure 2-16 shows the tapered design and its simulation result.

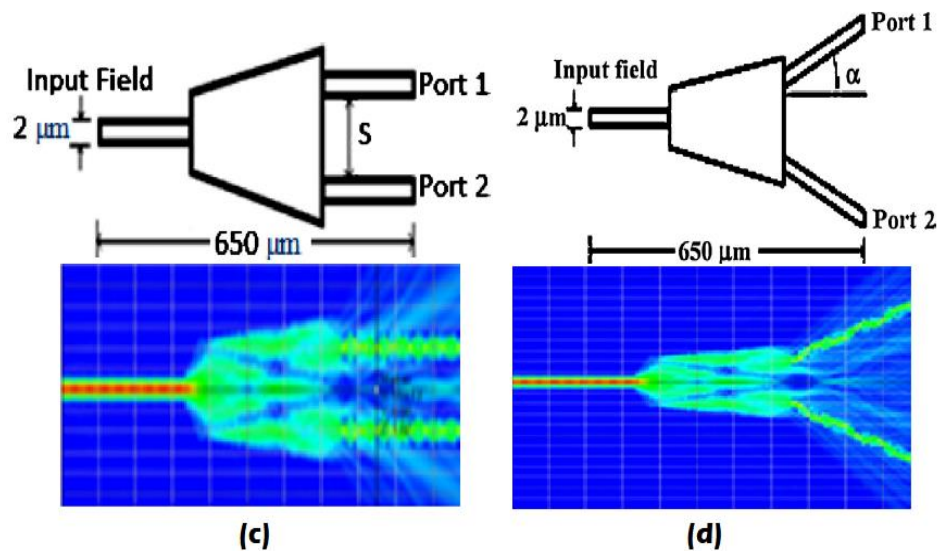


**Figure 2-16 : The tapered design and its simulation result (Chack et al., 2014).**

The maximum electric field intensity occurs when the separation distance is at an intermediate value. Furthermore, the electric field intensity is proportional to the arm length angle. The researcher summarizes that the tapered MMI structure performs better than the standard MMI structure. (Chack et al., 2014) also analyzed the effect of different input wavelength of MMI (1310nm and 1550nm). He also simulated the tapered structure in term of transverse electric (TE) and transverse magnetic (TM) polarizations. He also summarizes that varying the input wavelength significantly affects the insertion loss (IL) and extinction ratio (ER) and performs better than standard MMI structure. Table 2-3 shows the insertion loss (IL) and extinction ratio (ER).

**Table 2-3 : The insertion loss (IL) and Extinction ratio (ER)(Chack et al., 2015).**

(a) Wavelength, $\lambda = 1310$ nm			
Polarization	Output Parameter	Typical MMI	Tapered MMI
TE	IL (dB)	1.421	0.546
	ER (dB)	16.433	17.107
TM	IL (dB)	1.630	0.809
	ER (dB)	13.490	19.365
(b) Wavelength, $\lambda = 1550$ nm			
Polarization	Output Parameter	Typical MMI	Tapered MMI
TE	IL (dB)	0.857	0.255
	ER (dB)	11.288	19.487
TM	IL (dB)	0.677	0.482
	ER (dB)	14.970	23.394

#### 2.4.2 Parabolic Tapered MMI Coupler.

A parabolic tapered structure has been proposed by (Sahu, 2013) to improve the performance of multimode interference MMI coupler in Mach-Zehnder Interferometer (MZI) optical modulator. The design is based on the structure of a 2x2 symmetric coupler, as shown in Figure 2-17. The intention is to operate at a wavelength of  $1.55\mu\text{m}$  and was built upon SOI strip waveguides. The researcher designs a tapered MMI coupler of 3dB coupling length  $18.5\mu\text{m}$ . The simulation result also shows that the beat length ( $L\pi$ ) between TE and TM mode is 0.26% for both tapered. Whilst the other tapered design only obtains 0.25%. The Length ( $L\pi$ ) for p-value varying from 0.4 to  $w=1.5$ , cladding index=1.45 and separation between waveguide arm (h) is 2um, 3um and 4um.

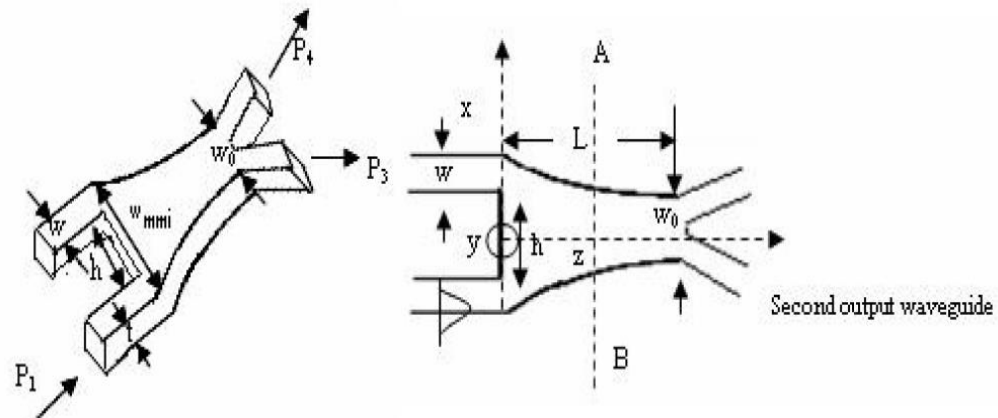


**Figure 2-17 : Proposed parabolic tapered structure of a 2x2 symmetric coupler (Sahu, 2013).**

The simulation result obtains from OptiBPM shows that the beat length ( $L$ ) of parabolic tapered MMI is half (0.5%) of the standard MMI structure for the same performance. With parabolic tapered, the incident angle reduces at each reflection on the core-cladding interface.

Figure 2-18 shows the 4X4 MMI parabolic tapered propose and designed by (Levy, 1998) in order to reduce MMI region size base on the principle of self-imaging, either general or restricted. General interference (GI) is stated to be independent of mode excitation, whereas restricted interference (RI) is solely dependent on mode excitation. Aside from the imaging type, it is recommended that the device's MMI design structure be tapered.



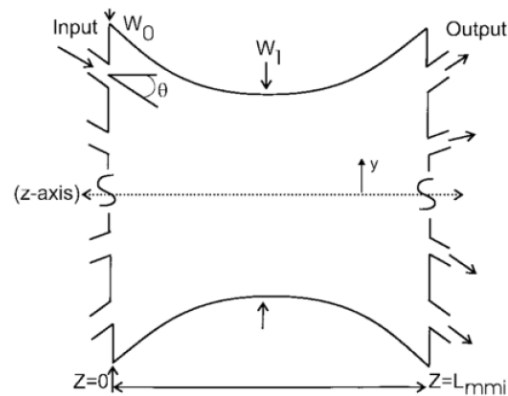


**Figure 2-18 : The 4X4 MMI parabolic tapered (Levy, 1998).**

The optical imaging across the device will be nearly along with the coordinate system, which is symmetrical referring to the end walls of the tapered MMI region if the input and output waveguides are tilted (Levy, 1998). This characteristic will significantly improve the output power and splitting ratio. The splitting ratio is a ratio between individual output port over the total waveguide output. With a region length half to the standard MMI structure, the splitting ratio varies between 23% to 27%, a  $\pm 2\%$  difference from the expected value of 25%.

Another researcher (Wei et al., 2001) shows interest in analyzing the effects of separating the output waveguide with S-bend tapered before connecting to MMI structures. The self-imaging fundamental has influenced the design characteristic of MMI devices. The design proposed is based on the structure of a 1x2 symmetric 3dB power splitter, as shown in Figure 2-19. The design parameter of the coupler is  $L=398\mu\text{m}$  and cross section at  $4.6\mu\text{m} \times 4\mu\text{m}$ , 5mm height of the Si top layer of the SOI, the etching depth is 2 mm.  $\omega_0=14.4$  mm,  $\omega_1=24$  mm, and  $\lambda=1.55$  mm.

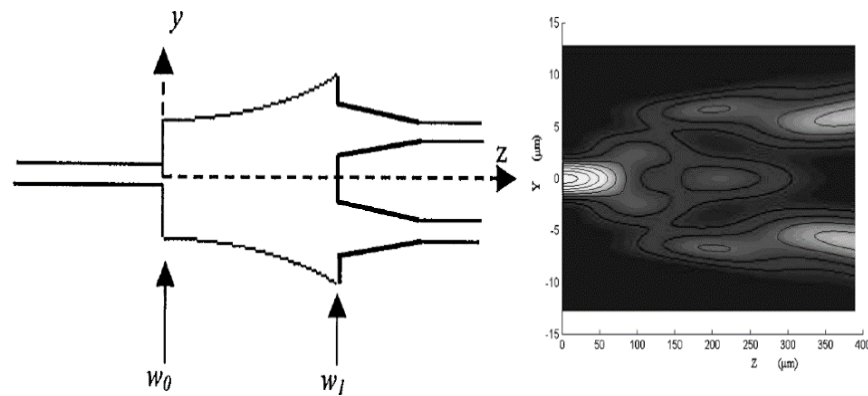


**Figure 2-19 : Parabolic tapered 1x2 symmetric 3dB power splitter (Wei et al., 2001).**

The simulation result signifies that the parabolic design with reducing MMI length gives better performance with the output uniformity of 0.28dB and excess loss of 9.9dB. The device's loss is measured using a power meter by patching a light throughout every output waveguide into a single-mode fiber. As the parabolic tapered MMI structure in the research is fabricated, the result obtained is more realistic as external effect and loss could happen.

UNIVERSITI TEKNIKAL MALAYSIA MELAKA

### 2.4.3 Exponential Tapered MMI Coupler.

An exponential tapered structure has been proposed by (J.-J. Wu, 2008) to improve the performance of multimode interference MMI coupler in Mach-Zehnder Interferometer (MZI) optical modulator. Although the parabolic tapered has a good performance as optical power splitter and compact in size, this researcher has proven that the exponential tapered can further reduce the length of this device. The design

proposed is based on the structure of a 1x2 symmetric power splitter, as shown in Figure 2-20.

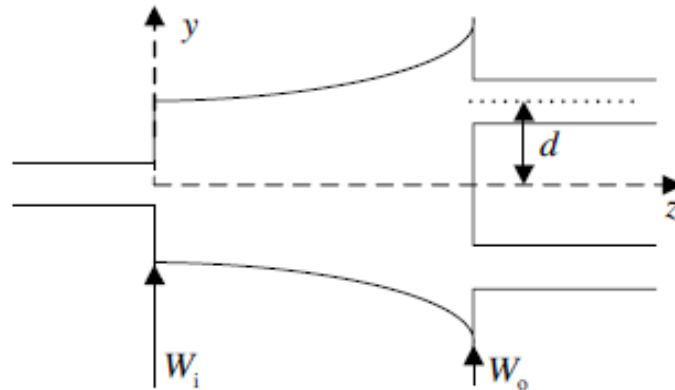


**Figure 2-20 : Exponential tapered 1x2 symmetric 3dB power splitter (J.-J. Wu, 2008).**

The performance of exponential tapered MMI structure in term of wavelength response, fabrication tolerance is investigated using 2D beam propagation method BPM. The exponential tapered is formulate according to,

$$W(z) = W_i + A \left( \exp \frac{gz}{L_{MMI}} \right) - 1$$

Where  $z$  is the direction of light propagation,  $L_{mmi}$  is length of region,  $W_i$  is the width of region. The simulation result shows that tapered structure has an effect to the imagine area. Furthermore, the summation of output power of exponentially tapered is larger than parabolic tapered. On the other hand, the wavelength response for each structure is the same.

## 2.5 Performance Evaluation Between Tapered Structure.

The performance of linear tapered and parabolic tapered has been analyzed by (Levy, 1998) through the beam propagation method (BPM). The research intention is to reduce the proximity limitation by separating the access waveguide. The researcher also employs the self-image property to maximize the design performance. The tapered MMI region is folded horizontal and vertically. Furthermore, the output waveguide is also tilted linear to the MMI region angle to equalize the input-output image. The tapered and non-tapered design share a common splitting ratio. The researcher summarizes that parabolic tapered has performed better in every test segment, as stated in Table 2-4.

**Table 2-4 : Linear and Parabolic performance analyzed by (Levy, 1998).**

	<b>Linear Tapered</b>	<b>Parabolic Tapered</b>
<b>Insertion loss</b>		0.8dB at 59% shorter
<b>Fabrication tolerance</b>	Lower	Higher
<b>Access waveguide</b>	Narrower	Wider
<b>Bending loss</b>	Higher	Lower

Another researcher (J.-J. Wu, 2008) propose an exponential tapered design and compared the design with parabolic tapered MMI structure. The performance is determined in term of dimension reduction, total optical transmission, fabrication tolerance and wavelength response. The performance parameter is generated from 2-Dimensional beam propagation method (BPM).

**Table 2-5 : Parabolic and Exponential performance compared by (J.-J. Wu, 2008).**

	<b>Exponential Tapered</b>	<b>Parabolic Tapered</b>
<b>Dimension</b>	Shorter	Longer
<b>Total power output</b>	Higher	Lower
<b>Transmission loss</b>	Lower	Higher
<b>Wavelength response</b>	Equal	

## 2.6 Design and Analysis Parameter of MMI Coupler.

Multimode interference (MMI) coupler is a compact and sensitive device. Most of the research focuses on reducing the size of MMI by modifying its structure and, at the same, maintains the performance. The MMI width and length are proportionate to each other. A researcher, (Soldano & Pennings, 1995) proposed that the length required for self-imaging is given by equation:

$$L\pi = \frac{4 nr We^2}{3 \lambda_o}$$

Where:

$nr$  = effective refractive index of wave guide.

$We$  = effective width of MMI region.

$\lambda_o$  = free space wavelength.

Self-imaging principles enable light to propagate in any number of modes which are referred to NxM MMI coupler. The performance of exponential tapered MMI structure in term of wavelength response, fabrication tolerance is investigated using 2D beam propagation method BPM. The exponential tapered is formulate according to:

$$W(z) = W_i + A \left( \exp \frac{gz}{L_{MMI}} \right) - 1$$

Where  $z$  is the direction of light propagation,  $L_{MMI}$  is length of region,  $W_i$  is the width of region. Some of important parameters to be considered in modeling difference tapered MMI couplers are extinction ratio (ER), insertion loss (IL), modulation efficiency (VL), length, and width (Razak et al., 2015). The insertion loss can be determined by the equation of:

$$I_L = 10 \log_{10} \frac{P_{in}}{P_{out}}$$

Where the  $P_{in}$  is the power input and  $P_{out}$  is the output power. In the beam propagation method software, the analysis can be computes automatically. The performance of MMI coupler also can be verified in term of modulation efficiency given by the equation of:

$$\text{Modulation efficiency} = V\pi L\pi$$

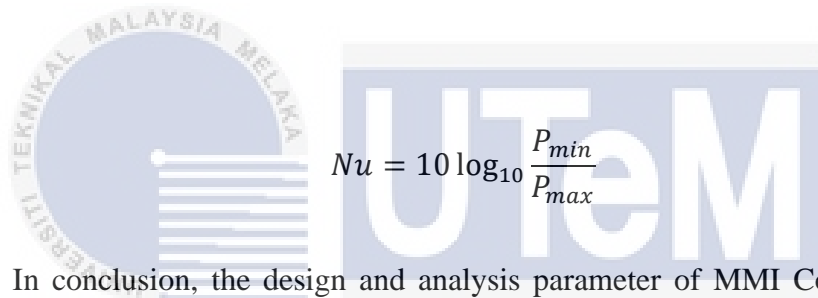
$$L_\pi = \frac{\Delta\phi\lambda}{2\pi\Delta n}$$

The value of  $V\pi$  is taken from the voltage of the active region of the phase modulator.

Where,  $\Delta\phi$  is the phase shift and  $\Delta n$  is the refractive index rate of change. While  $\lambda$  is the wavelength of the signal. The data such as extinction ratio (ER), free space range (FSR) and  $\Delta\lambda$  can be obtain directly from a waveform. By manipulation, the parameter as mentioned above the phase shift can be calculated by the formula,

$$\Delta\phi = \frac{2\pi\Delta nL}{FSR}$$

Another researcher (Shi et al., 2005) stated that the best design of MMI coupler can be determine by insertion loss (IL) and also non-uniformity that can be define by,



$$Nu = 10 \log_{10} \frac{P_{min}}{P_{max}}$$

In conclusion, the design and analysis parameter of MMI Coupler aims as discussed above is to obtain the best performance by comparing between each design. The design was studied based on signal-to-noise ratio (SNR) and the characteristic is shown in Table 2-6.

**Table 2-6 : Signal to Noise Ratio comparison between output parameters.**

<b>Output Parameters</b>	<b>S/N Ratio</b>
<b>Insertion loss, IL</b>	The smaller the better
<b>Extinction ratio, ER</b>	The larger the better
<b>Modulation efficiency</b>	The smaller the better

## CHAPTER 3

### METHODOLOGY



This project comprises two main focuses, modelling difference tapered structure of multimode interference (MMI) and then comparing the performance of each design. All the modelling dan testing will be done using beam propagation method software (OptiBPM). The structure design will focus on the different tapered type on the input and output waveguide of the NxM 1x2 power splitter multimode interference (MMI) coupler. The three (3) main tapered structure is as shown in the Figure 3-1.



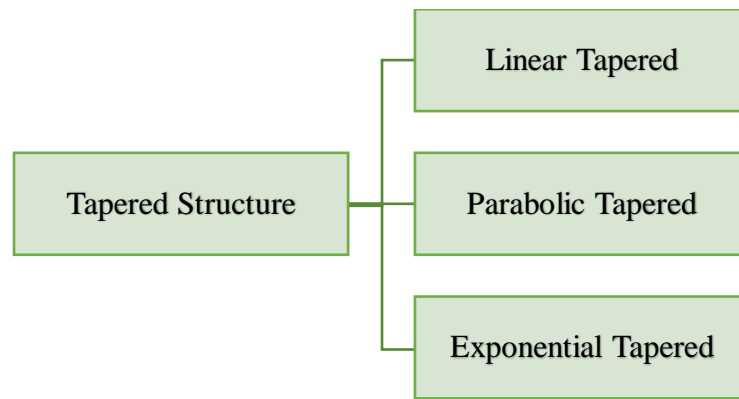


**Figure 3-1 : The three (3) primary tapered structure.**

After completing the modelling of 1x2 power splitter multimode interference (MMI) coupler, the research continues to simulate each design. This is the crucial part of the research to determine the functionality of the design. Important parameter generated from the simulation process will be gathered and manipulate to determine the insertion loss (IL) produces by each design. The modification is made to the tapered design if the performance is not exceeding the expected level. Figure 3-2 displays the flowchart of the research methodology to clarify the direction of this project. A detailed explanation is attached with the flowchart.

### **3.1 Project Planning and Gantt Chart.**

The completion of a project depends on how the source and time are managed. One of the best tools to oversee every aspect of this project is the Gantt chart. In this chart, all the project schedule and task are listed to have complete knowledge of the project's timeline (Refer Appendix A).

### 3.2 Research Methodology Flowchart.

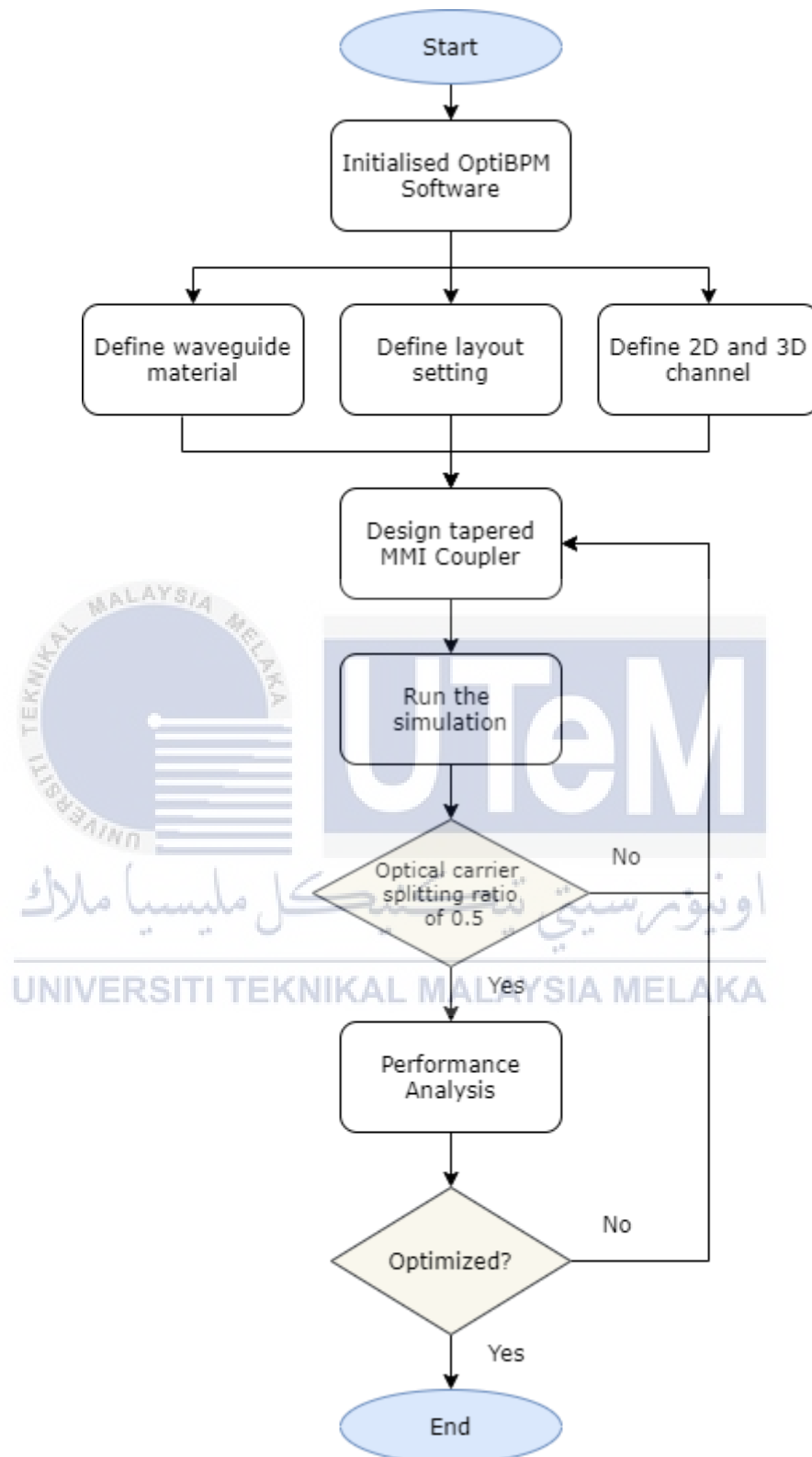


Figure 3-2 : Research methodology flowchart.

### 3.3 Detail Description of The Research Methodology Flowchart.

Certain procedures must be followed to carry out and execute the project to ensure the job is finished within the time allocated.

The OptiBPM software is initialised with the feature configuration on designing the waveguide coupler. The first parameter to be set in OptiBPM GUI is defining the waveguide material, including the 2D-3D wafer properties, refractive index, and dielectric. Next, the 2D and 3D channel profiles are defined and if the 2D simulator is called, any point inside a waveguide associated with the profile name will have the same refractive index. The layout setting windows is where the detail dimension of MMI coupler is set, such as the waveguide width, wafer dimension, 2D wafer properties, 3D wafer properties, and finally store all the design setting as *.bpd* files.

The 2D design starts with sketching the desired tapered structure of MMI Coupler in project layout windows. Parameters and the dimension of tapered MMI coupler are set according to the theoretical design dimension base on the mathematical formulation. Before the simulation can be made, the input plane must be set at the waveguide input arm. The process continues with the simulation of the design structure, where the simulation parameters are set to 2D Isotropic simulation. The first stage of the simulation is for confirmation that the design structure achieved the optical carrier splitting ratio of 0.5. If the value is not exceeding the targeted ratio, the modification to the design structure must be made.

The tapered structure of the MMI coupler is analysed from the data generated by OptiBPM analyser tools such as optical field propagation, refractive index

propagation, and cut view. In this stage, the output simulation will be analysed compared to the theoretical design, whether it matches or gives specific new results. If the result does not meet the minimum requirement, theoretical calculation and tapered modification will be made to improve the performance.

Finally, the performance of each tapered structure will be documented for the verification process.

### 3.4 Multimode Interference (MMI) Coupler Design Parameters.

Multimode interference (MMI) coupler is a compact and sensitive device. Most of the research focuses on reducing the size of MMI by modifying its structure and, at the same, maintains the performance. The MMI width and length as illustrates in Figure 3-3 are proportionate to each other. A researcher, (Soldano & Pennings, 1995) proposed that the length required for self-imaging is by,

$$L\pi = \frac{4nrWe^2}{3\lambda_0}$$

Where:

$nr$  = effective refractive index of wave guide.

$We$  = effective width of MMI region.

$\lambda_0$  = free space wavelength.

The basic design of a 1x2 MMI coupler without tapering the input/output waveguide is illustrated in Figure 3-3. At the same time, the creation of MMI coupler with tapering input/output waveguide is shown in Figure 3-4 and Figure 3-5.

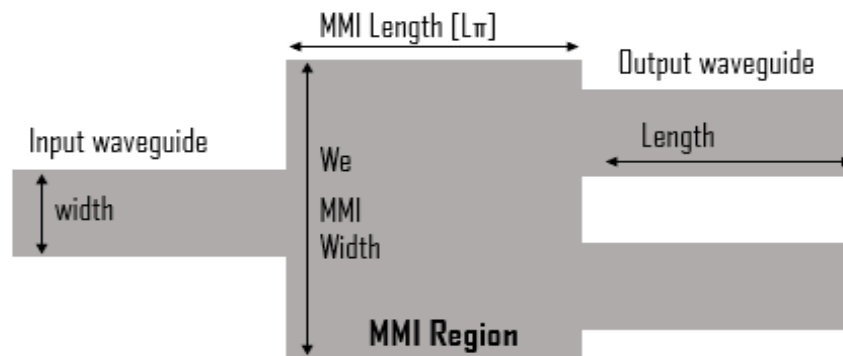


**Figure 3-3 : 1x2 MMI power splitter.**

Self-imaging principles enable light to propagate in any number of modes which are referred to NxM MMI coupler. The performance of exponential tapered MMI structure in term of wavelength response, fabrication tolerance is investigated using 2D beam propagation method BPM. The exponential tapered is formulate according to the given equation:

$$W(z) = W_i + A \left( \exp \frac{gz}{L_{MMI}} \right) - 1$$

Where  $z$  is the direction of light propagation,  $L_{MMI}$  is length of region,  $W_i$  is the width of region. Some of important parameters to be considered in modeling difference tapered MMI couplers are extinction ratio (ER), insertion loss (IL), modulation efficiency (VL), length, and width (Razak et al., 2015). The insertion loss can be determined by the equation:

$$I_L = 10 \log_{10} \frac{P_{in}}{P_{out}}$$

Where the  $P_{in}$  is the power input and  $P_{out}$  is the output power. In the beam propagation method software, the analysis can be computed automatically.

Another researcher (Shi et al., 2005) stated that the best design of MMI coupler can be determine by insertion loss (IL) and also non-uniformity that can be defined by,

$$Nu = 10 \log_{10} \frac{P_{min}}{P_{max}}$$

The performance of MMI coupler also can be verified in term of modulation efficiency given by the equation:

$$\text{Modulation efficiency} = V\pi L\pi$$

$$L_{\pi} = \frac{\Delta\phi\lambda}{2\pi\Delta n}$$

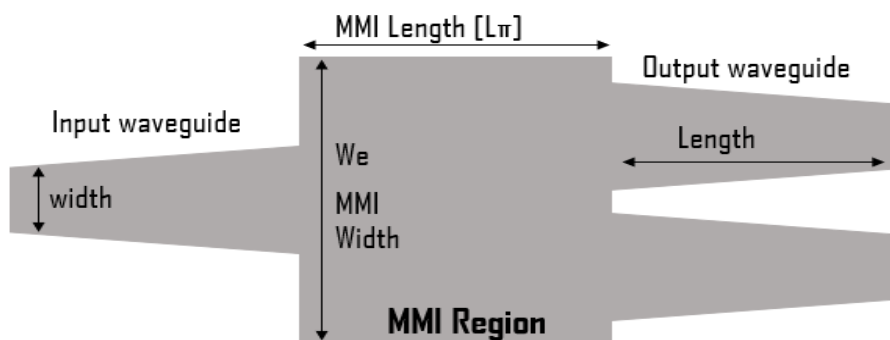


**Figure 3-4 : Linear tapered MMI diagram.**

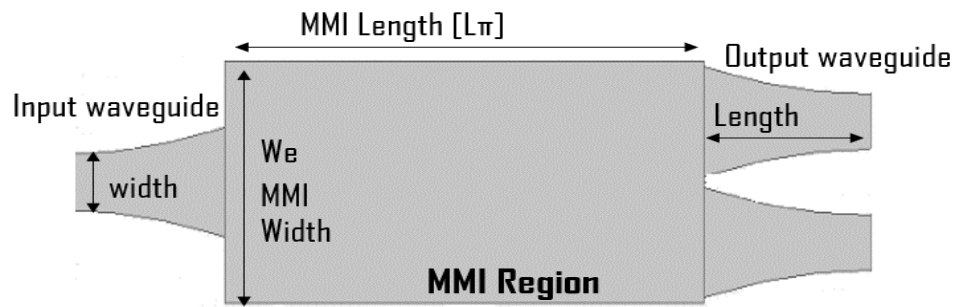


**Figure 3-5 : Parabolic tapered MMI diagram.**

Table 3-1 displays the crucial parameter for designing and modelling the different tapered structure of MMI coupler. All design in this project will employ the same parameter as stated in the table.

Parameter	Value
MMI width [ $\mu\text{m}$ ]	22, 26, 30, 34, 38
MMI length [ $\mu\text{m}$ ]	To be determine from formulation.
Input waveguide width [ $\mu\text{m}$ ]	2 to 4
Input waveguide length [ $\mu\text{m}$ ]	200
Output waveguide width [ $\mu\text{m}$ ]	2 to 4
Output waveguide length [ $\mu\text{m}$ ]	200
Waveguide refractive index	3.45
Cladding refractive index	1.0
Wavelength [ $\mu\text{m}$ ]	1.55

### 3.5 Simulation of Multimode Interference (MMI) Coupler.

The different tapered structure of multimode interference (MMI) coupler is modelled using OptiBPM, a 2-dimensional beam propagation method software by Optiwave Corporation. The software uses a mathematical manipulation equation Helmholtz approximation as its propagation models to allow light propagation in a dielectric medium. The equation can simplify the simulations, reduce the processing time and for better computer memory management. The design of waveguide structure can be done conveniently, fast and with high accuracy as it uses a computer-aided design environment (CAD). Some of the feature offered by this software is very useful and customizable. A designer can set and modify the polarization, boundary condition and refractive index.

The software simulates optical propagation in two-dimensional (2D) and three-dimensional (3D) modes. In 2D mode, the X-axis is for vertical (transverse), and the Z-axis is for horizontal (propagation). Whilst, for the 3D mode, the X-axis is for the vertical (transverse), Y-axis (depth) and Z-axis is set for horizontal (propagation).

The 2D BPM simulator uses Crank-Nicolson method that works on the unconditionally stable finite difference algorithm. Therefore, customizing can be made between TE and TM polarization and Pade approximants of wide-angle propagation depending on the design. In addition, another aspect that can be custom are starting field choice as a waveguide mode, a user field, a Gaussian field, and a rectangular field. Figure 3-6 illustrates the four (4) main applications in OptiBPM software.



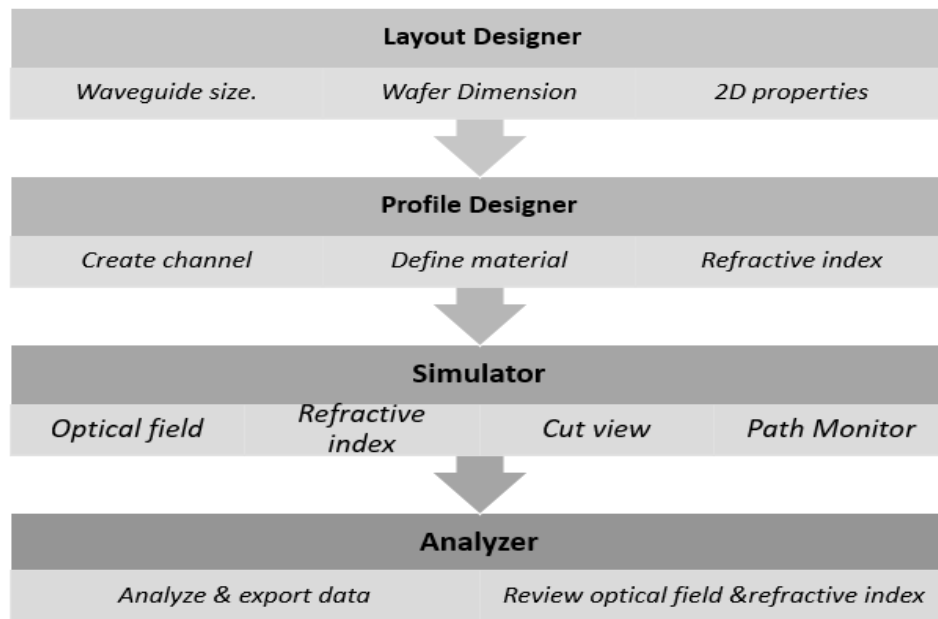


**Figure 3-6 : Illustration of the four (4) main application in OptiBPM software.**

The process of creating and simulation the multimode interference (MMI) coupler in OptiBPM must undergo a step-by-step procedure. It is very crucial to determine all the important parameter is defined accordingly to produce an accurate result. Figure 3-7 shows the design and simulation process.

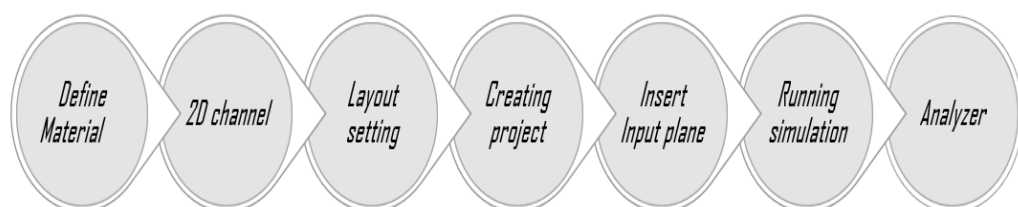


**Figure 3-7 : The process of designing and simulation in OptiBPM.**

Although this research intends to model different tapered structure of multimode interference (MMI) coupler, some standard parameters need to be defined to ease the performance comparison. Table 3-2 displays the common simulation parameter for all design in this research.

**Table 3-2 : Common simulation parameter for all design.**

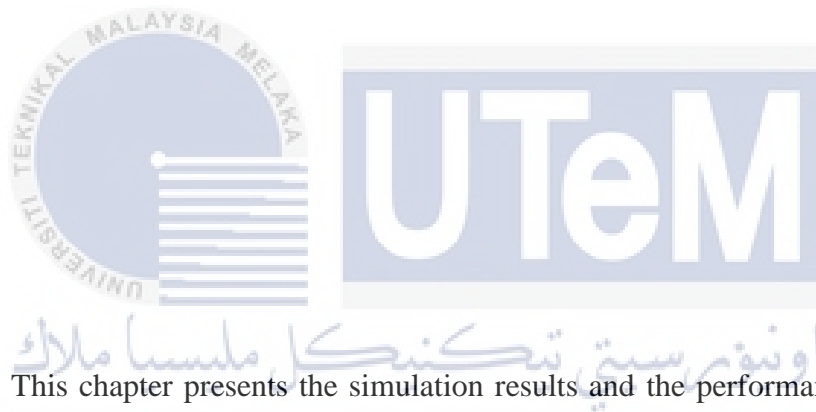
<b>Parameter</b>	<b>Value</b>
<b>Waveguide refractive index</b>	3.45
<b>Cladding refractive index</b>	1.0
<b>Wavelength (nm)</b>	1500
<b>Reference Index</b>	Mod
<b>Polarization</b>	TE
<b>BPM Solver</b>	Paraxial
<b>Boundary condition</b>	TBC

اونيورسيتي تيكنيكل مليسيا ملاك

UNIVERSITI TEKNIKAL MALAYSIA MELAKA

## CHAPTER 4

### RESULTS AND DISCUSSION



This chapter presents the simulation results and the performance analysis of different tapered structures of multimode interference (MMI) coupler. The simulation work was implemented using OptiBPM version 12, a waveguide optics design software produced by Optiwave System Inc. The effect on MMI performance by varying MMI width, MMI length dan also tapering the input/output waveguide is presented and discussed in output power and insertion loss (IL).

The design for 1x2 MMI coupler is based on several fixed parameters such as MMI region (width and length), waveguide (input and output) width, waveguide (input and output) length, refractive index, and wavelength. The 1x2 MMI Coupler modelling process is performed on the waveguide layout designer tools. Next, the quality and accuracy of the design were determined using 2D simulation tools and

analyzer tools. Among the observations are optical field propagation (XZ slice), refractive index propagation (XZ slice), cut view and output power. Table 4-1 displays the design parameter of MMI coupler for non-tapered, linear tapered, parabolic tapered and exponential tapered.

**Table 4-1: The design parameter of MMI coupler.**

Parameter	Value
MMI width [ $\mu\text{m}$ ]	22, 26, 30, 34, 38
MMI Length [ $\mu\text{m}$ ]	545, 750, 1060, 1300, 1600
Waveguide width [ $\mu\text{m}$ ]	2, 4
Guide refractive index	3.45
Cladding refractive index	1.00
Wavelength	1.55 $\mu\text{m}$

#### 4.1 Non-tapered MMI coupler.

At the initial stage, the basic design of 1x2 MMI coupler without tapering the input and output waveguide is created based on five structure widths, 22  $\mu\text{m}$ , 26  $\mu\text{m}$ , 30  $\mu\text{m}$ , 34  $\mu\text{m}$  and 38  $\mu\text{m}$ . At the same time, the length of each design is set depending on the self-imaging principle and its formula. This basic design is essential for comparing and analyzing non-tapered MMI and tapered MMI structures. The detail parameter of 1x2 non-tapered MMI Coupler can be referred at Table 4-1.

The quality and performance of each design are determined based on an output splitting ratio of 0.5, where the equivalent splitting occurs at the coupler output. Measurements of output power splitting ratio were obtained from OptiBPM Analyzer. The designed structure of 1x2 MMI coupler with a width of  $30\ \mu\text{m}$  and length of  $1300\ \mu\text{m}$  is presented in Figure 4-1, while the simulation of optical field propagation (XZ Slice) is displayed in Figure 4-2.

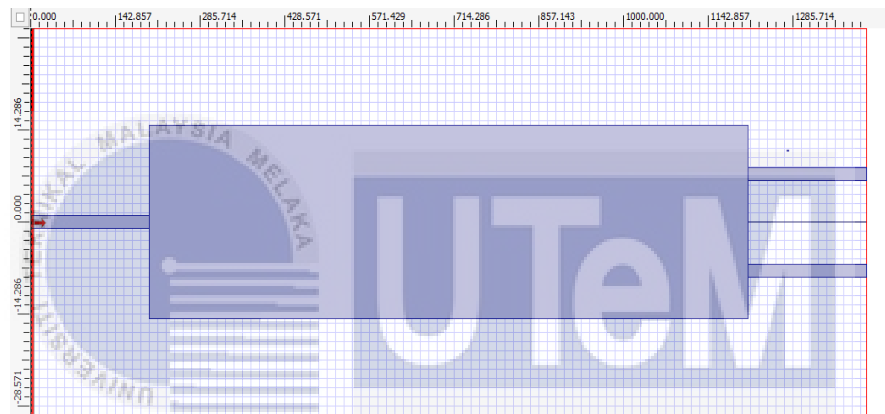


**Figure 4-1: 1x2 MMI Coupler structure in OptiBPM Designer, width= $30\ \mu\text{m}$ .**

UNIVERSITI TEKNIKAL MALAYSIA MELAKA

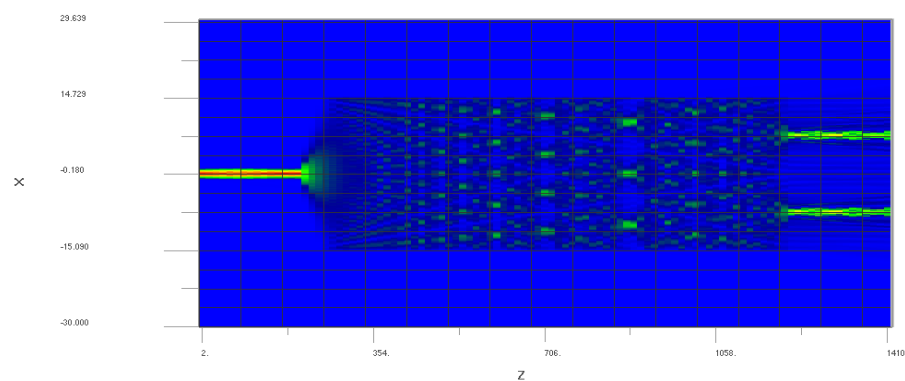


**Figure 4-2: Optical field propagation of 1x2 MMI Coupler in OptiBPM Analyzer, width= $30\ \mu\text{m}$ .**

After completing the 1x2 MMI Coupler design, the output power ratio of non-tapered MMI can be analyzed as illustrated in Figure 4-3. The output power shown in Figure 4-3 is the combination of both output arms. The result shows that the MMI coupler with a width of 30  $\mu\text{m}$  has achieved the highest splitting ratio, providing optimal power output. Next, the insertion loss for each design is calculated, as shown in Figure 4-4. Based on the line graph, the MMI Coupler design with a width between 22 to 30  $\mu\text{m}$  has an insertion loss between 1.6 dB to 2 dB. The rate begins to increase for MMI widths exceeding 30  $\mu\text{m}$ .

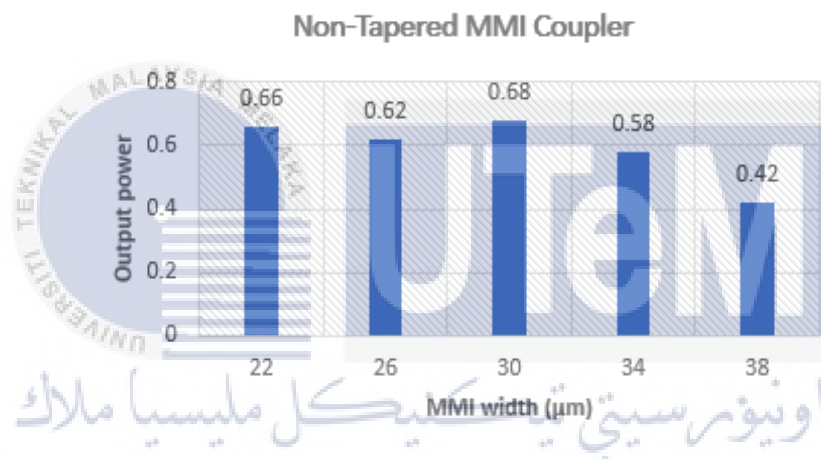


Figure 4-3: Non-tapered MMI Coupler output power.

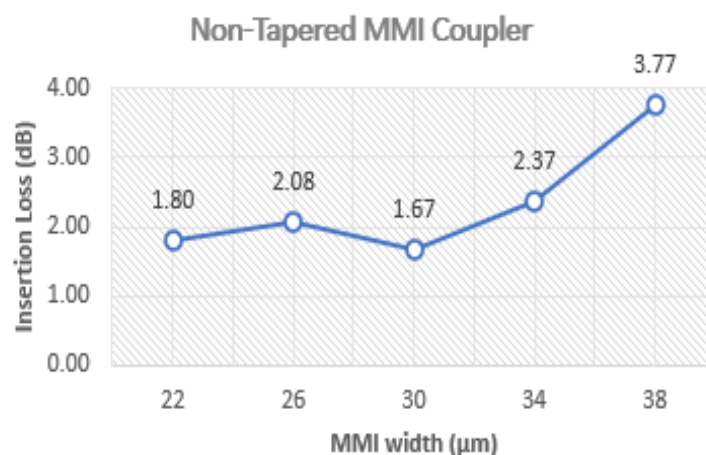


Figure 4-4: Non-tapered MMI Coupler insertion loss (IL).

## 4.2 Linear Tapered MMI Coupler.

Linear tapered MMI coupler are among the earliest tapering models proposed by researchers. A linear tapered structure has been proposed by (Thomson et al., 2010) to improve the performance of multimode interference MMI coupler in Mach-Zehnder Interferometer (MZI) optical modulator. The design is based on the structure of a 1x2 symmetric MMI Coupler, as shown in Figure 4-5. The MMI Coupler is created based on five structure widths, 22  $\mu\text{m}$ , 26  $\mu\text{m}$ , 30  $\mu\text{m}$ , 34  $\mu\text{m}$  and 38  $\mu\text{m}$ . At the same time, the length of each design is set depending on the self-imaging principles.

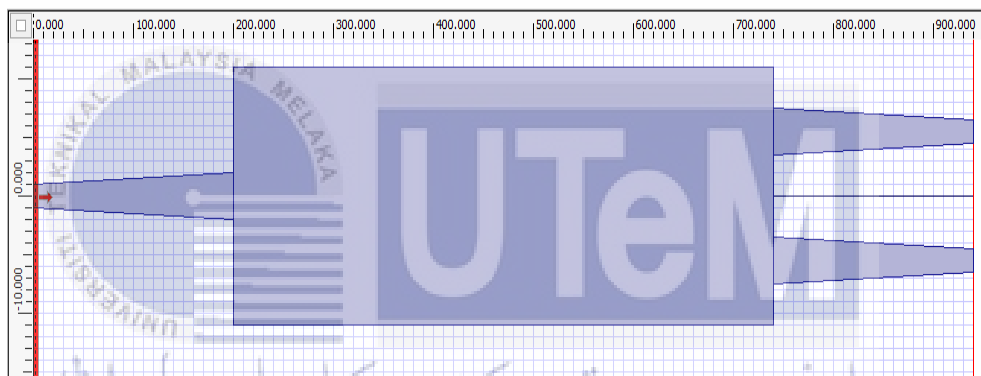


Figure 4-5: Linear tapered 1x2 MMI Coupler structure in OptiBPM Designer, width=22  $\mu\text{m}$ .

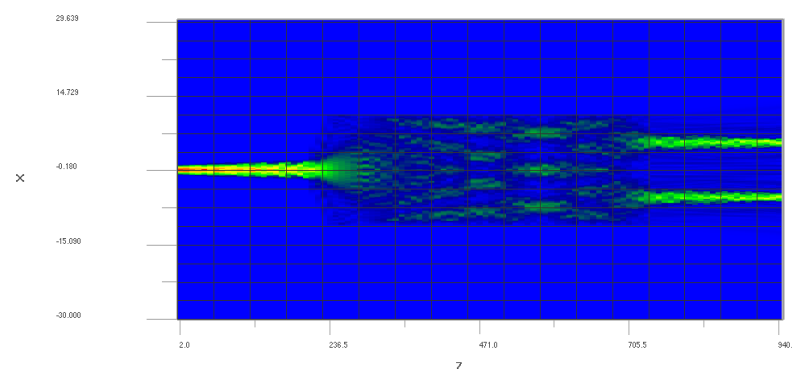
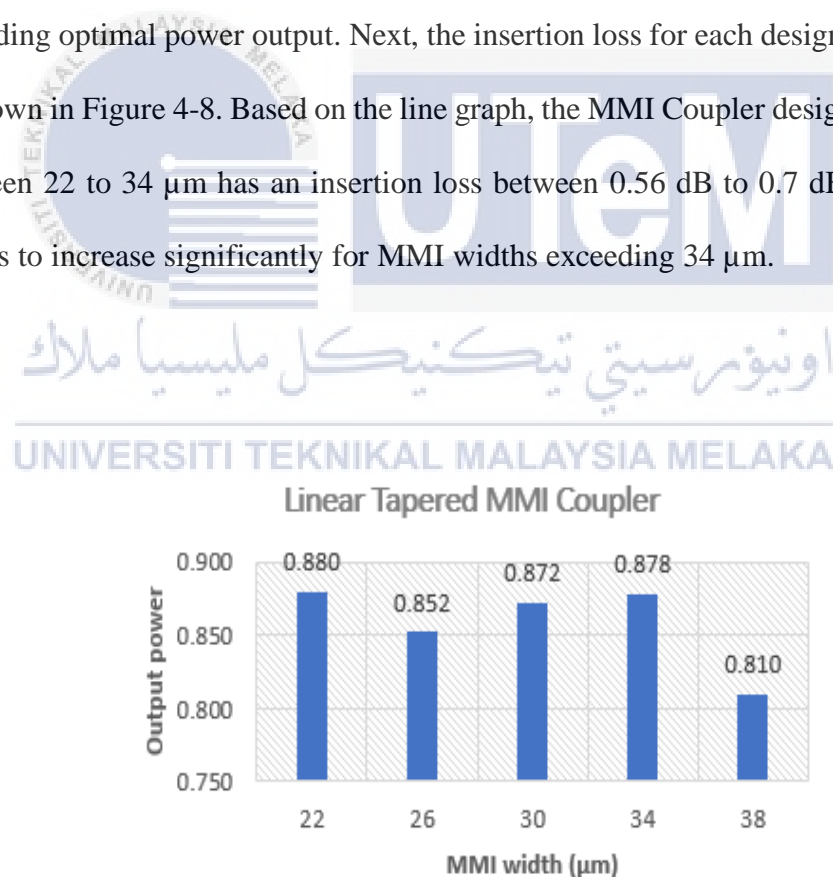


Figure 4-6: Optical field propagation of linear tapered 1x2 MMI Coupler in OptiBPM Analyzer, width=22  $\mu\text{m}$ .

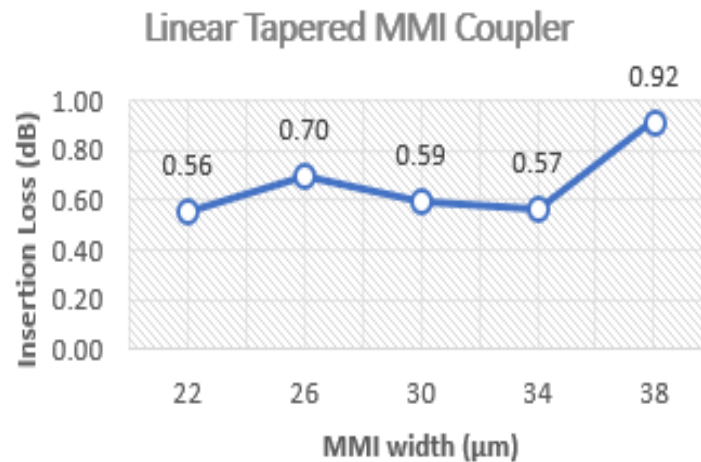
The quality and performance of each design are determined based on an output splitting ratio of 0.5, where the equivalent splitting occurs at the output splitter. Measurements of output power splitting ratio were obtained from OptiBPM Analyzer. The MMI Coupler with a dimension of 22  $\mu\text{m}$  wide and 545  $\mu\text{m}$  long is presented in Figure 4-5, while the simulation of optical field propagation (XZ Slice) is displayed in Figure 4-6 .

Figure 4-7 illustrates the output power ratio of linear tapered MMI. The output power shown is the combination of both output arms. The results show that the MMI Coupler design with a width of 22  $\mu\text{m}$  has achieved the highest splitting ratio, providing optimal power output. Next, the insertion loss for each design is calculated, as shown in Figure 4-8. Based on the line graph, the MMI Coupler design with a width between 22 to 34  $\mu\text{m}$  has an insertion loss between 0.56 dB to 0.7 dB. But the rate begins to increase significantly for MMI widths exceeding 34  $\mu\text{m}$ .



**Figure 4-7: Linear tapered MMI Coupler output power.**





**Figure 4-8: Linear tapered MMI Coupler insertion loss (IL).**

### 4.3 Parabolic Tapered MMI Coupler.

Parabolic tapered MMI coupler is popular and widely used nowadays to improve the performance of multimode interference MMI coupler in Mach-Zehnder Interferometer (MZI) optical modulator. The design is based on the structure of a 1x2 symmetric MMI Coupler, as shown in Figure 4-9. The parabolic tapered of MMI Coupler is created based on five structure widths, 22  $\mu\text{m}$ , 26  $\mu\text{m}$ , 30  $\mu\text{m}$ , 34  $\mu\text{m}$  and 38  $\mu\text{m}$ . At the same time, the length of each design is set depending on the self-imaging principles.

The simulation of optical field propagation (XZ Slice) for MMI Coupler with a dimension of 26  $\mu\text{m}$  wide and 750  $\mu\text{m}$  long is presented in Figure 4-10. The quality and performance of each design are determined based on an output splitting ratio of 0.5, where the equivalent splitting occurs at the output splitter. Measurements of output power splitting ratio were obtained from OptiBPM Analyzer.

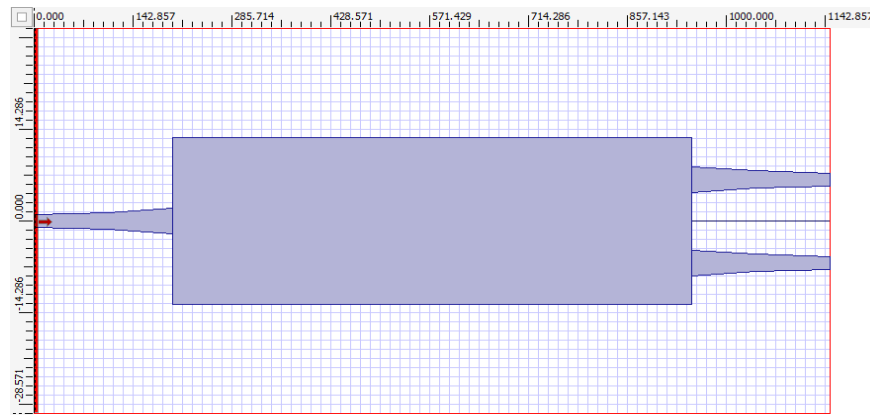


**Figure 4-9: Parabolic tapered 1x2 MMI Coupler structure in OptiBPM Designer, width=26  $\mu\text{m}$ .**

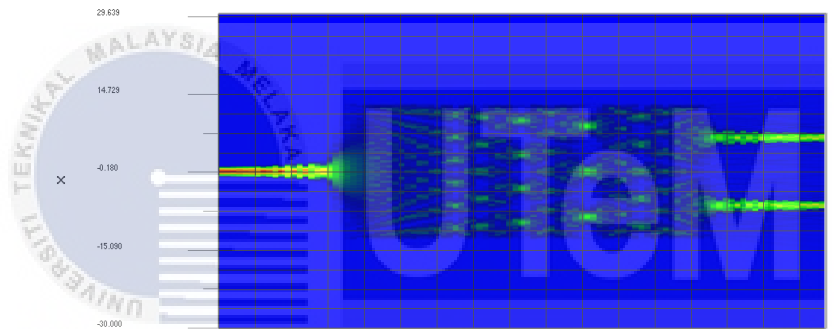


**Figure 4-10: Optical field propagation of parabolic tapered 1x2 MMI Coupler in OptiBPM Analyzer, width=26  $\mu\text{m}$ .**

The output power ratio for various widths of parabolic tapered MMI has been analyzed and recorded, as illustrated in Figure 4-11. The output power is the total power in both output arms. The results obtained show that the MMI coupler design with a width of 26  $\mu\text{m}$  has achieved the highest splitting ratio, providing optimal power output. Next, the insertion loss for each design is calculated, as shown in Figure 4-12. Based on the line graph, the MMI splitter design with a width between 22 to 26  $\mu\text{m}$  has an insertion loss less than 0.5 dB. The rate begins to increase significantly for MMI widths exceeding 30  $\mu\text{m}$ .

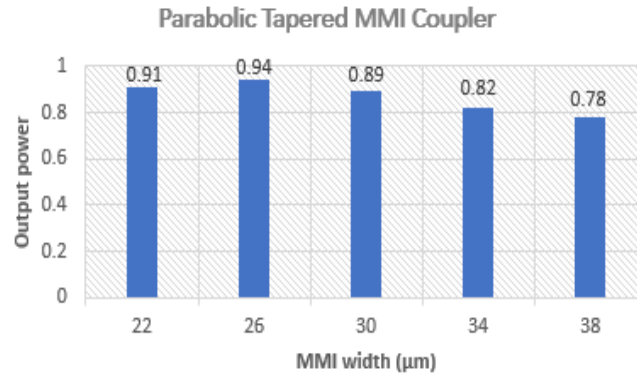


Figure 4-11: Parabolic tapered MMI Coupler output power ratio.

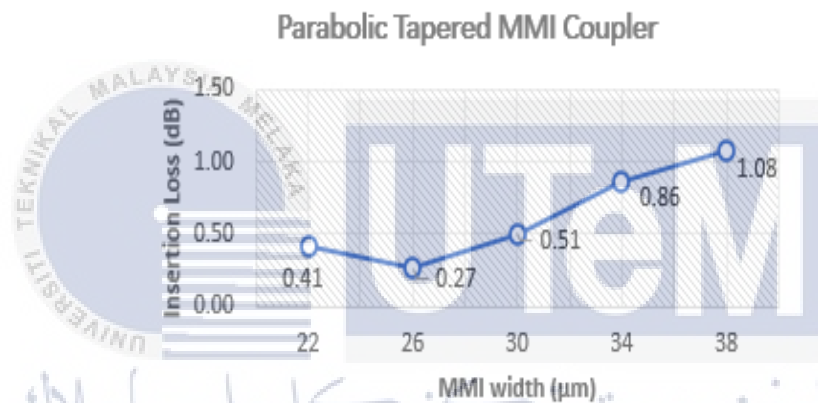
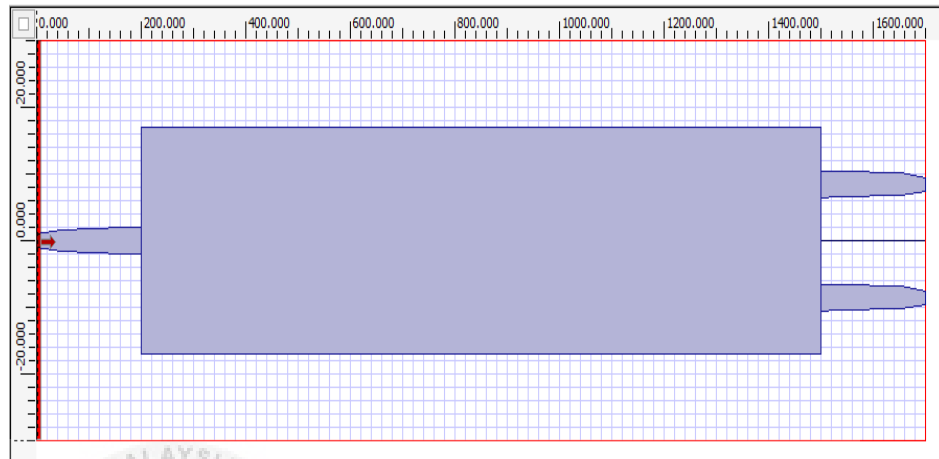


Figure 4-12: Parabolic tapered MMI Coupler insertion loss (IL).

#### 4.4 Exponential Tapered MMI Coupler.

Another approach in tapering the input and output of MMI coupler is exponential tapered. The design is based on the structure of a 1x2 MMI coupler with the width of 22  $\mu\text{m}$ , 26  $\mu\text{m}$ , 30  $\mu\text{m}$ , 34  $\mu\text{m}$  and 38  $\mu\text{m}$ . At the same time, the length of each design is set depending on the self-imaging principles.

The designed structure of MMI Coupler with a dimension of  $34\ \mu\text{m}$  wide and  $1300\ \mu\text{m}$  long is presented in Figure 4-13, while the simulation of optical field propagation (XZ Slice) is displayed in Figure 4-14.



**Figure 4-13: Exponential tapered 1x2 MMI Coupler structure in OptiBPM Designer, width= $34\ \mu\text{m}$ .**

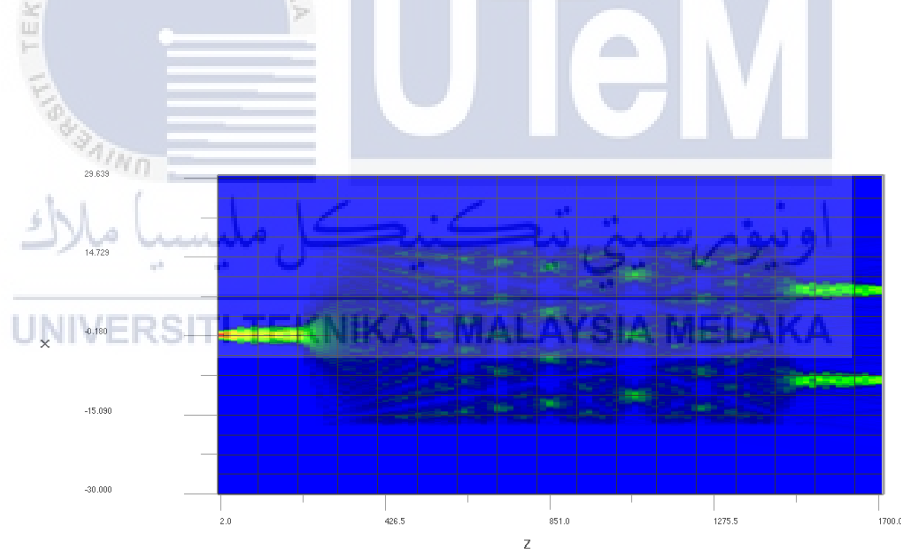


**Figure 4-14: Optical field propagation of exponential tapered 1x2 MMI Coupler in OptiBPM Analyzer, width= $34\ \mu\text{m}$ .**

Figure 4-15 illustrates the output power ratio of exponential tapered MMI. The output power is the total power in both output arms. The results show that the MMI splitter design with a width of  $34\ \mu\text{m}$  has achieved the highest splitting ratio, providing

optimal power output. Next, the insertion loss for each design is calculated, as shown in Figure 4-16. Based on the line graph, the MMI splitter design with a width of 22  $\mu\text{m}$  to 34  $\mu\text{m}$  has an insertion loss between 0.34 dB to 0.41 dB. On the other hand, the rate begins to increase significantly for MMI widths exceeding 34  $\mu\text{m}$ .

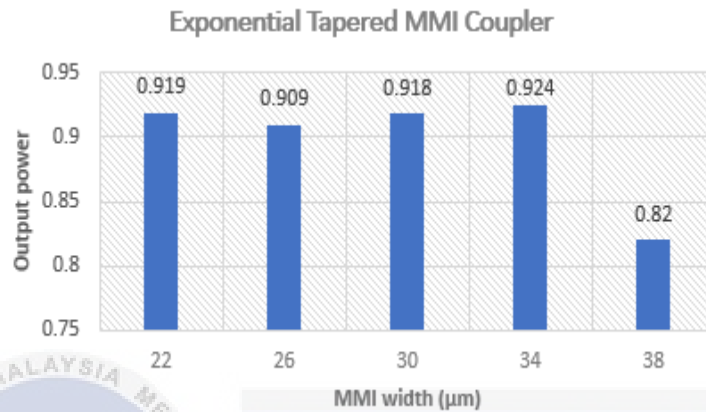


Figure 4-15: Exponential tapered MMI Coupler output power ratio.

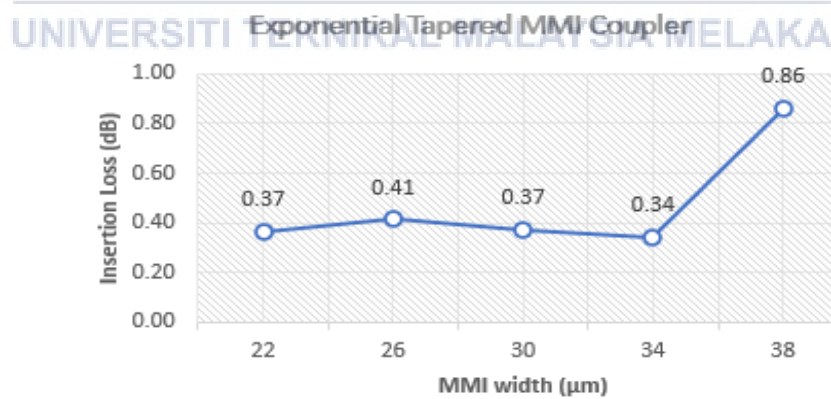


Figure 4-16: Exponential tapered MMI Coupler insertion loss (IL).

#### 4.5 Symmetrical Tapered MMI Coupler.

The symmetrical tapered MMI region structure is developed based on a series of prism sections combination. Five (5) MMI couplers were models with different width combinations to compare the performance. Table 4-2 displays the design parameter. The maximum electric field intensity occurs when the separation distance of the output waveguide is at an intermediate value.

**Table 4-2: The design parameter of symmetrical tapered MMI coupler**

Parameter	Value
MMI width [ $\mu\text{m}$ ]	11 to 22, 13 to 26, 15 to 30, 17 to 34 and 19 to 38
MMI length [ $\mu\text{m}$ ]	278, 385, 518, 660, 820
Waveguide width [ $\mu\text{m}$ ]	2
Guide refractive index	3.45
Cladding refractive index	1.00
Wavelength	1.55 $\mu\text{m}$

The designed structure of 1x2 symmetrical tapered MMI splitter with a width expands from 11  $\mu\text{m}$  to 22  $\mu\text{m}$  and 278  $\mu\text{m}$  long is presented in Figure 4-17, while the simulation of optical field propagation (XZ Slice) is displayed in Figure 4-18.

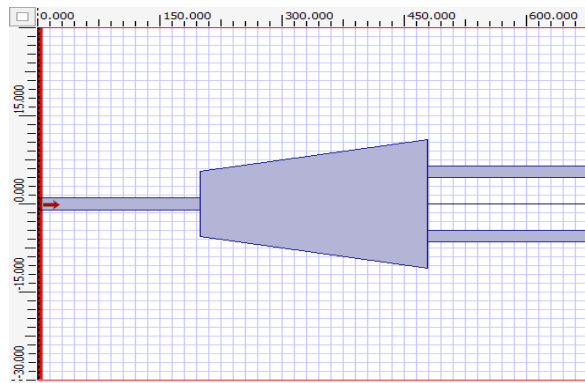


**Figure 4-17: Symmetrical tapered 1x2 MMI Coupler structure in OptiBPM Designer, width=11 to 22  $\mu\text{m}$ .**

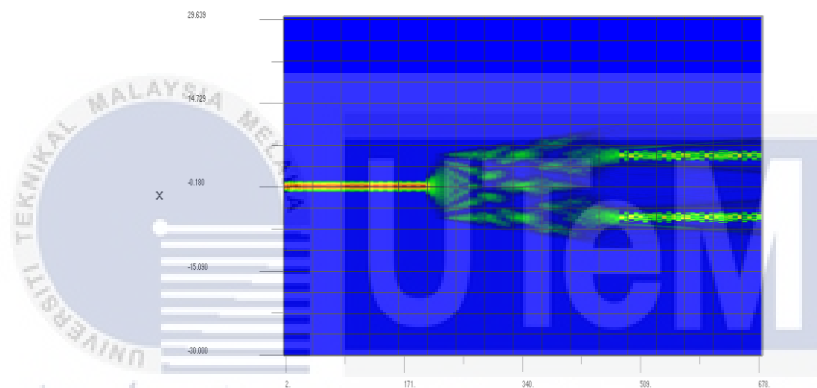


**Figure 4-18: Optical field propagation of symmetrical tapered 1x2 MMI Coupler in OptiBPM Analyzer, width=11 to 22  $\mu\text{m}$ .**

The output power ratio for various widths of symmetrical tapered MMI has been analyzed and recorded, as illustrated in Figure 4-19. The output power is the total power in both output arms. The results shows that the MMI splitter with a width of expand from 11  $\mu\text{m}$  to 22  $\mu\text{m}$  has achieved the highest splitting ratio, providing optimal power output. Next, the insertion loss for each design is calculated, as shown in Figure 4-20. Based on the line graph, the insertion loss is ranged between 1.38 dB to 1.97 dB.

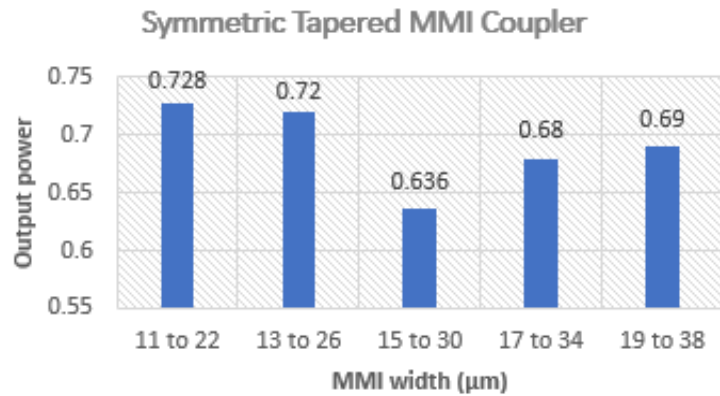


**Figure 4-19: Symmetrical tapered MMI Coupler output power ratio.**

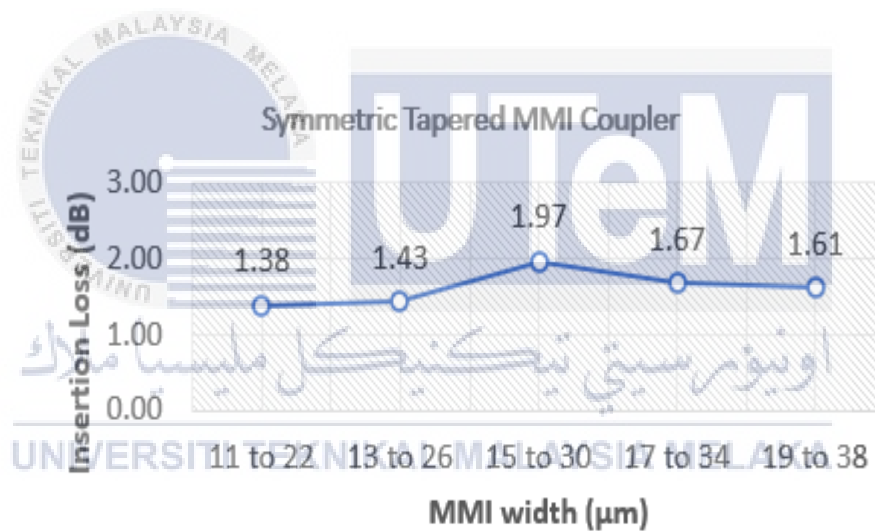


**Figure 4-20: Symmetrical tapered MMI Coupler insertion loss (IL).**



#### 4.6 Input/Output Waveguide Tapered Width.

The resultant from a recent research paper, as mentioned in Chapter 2, has shown that tapering at the input and output waveguide of MMI significantly improves the extinction ratio, reducing loss and minimizing the size of the optical devices. Therefore, the appropriate tapering size is critical for optimal MMI coupler performance. Therefore, the right tapering size is vital for optimal MMI coupler performance. Four (4) different sizes of input and output waveguide width were designed and simulated to analyze the impact of increasing the tapering size. Table 4-3 displays the design parameter of parabolic tapered MMI coupler.

**Table 4-3: The design parameter of parabolic tapered MMI coupler.**

Parameter	Value
MMI width [ $\mu\text{m}$ ]	26
Waveguide width [ $\mu\text{m}$ ]	2 to 4, 2 to 6, 2 to 8, 2 to 10
Guide refractive index	3.45
Cladding refractive index	1.00
Wavelength [ $\mu\text{m}$ ]	1.55

The parabolic tapered was chosen in this analysis because this design has shown the best performance in terms of insertion loss. The designed structure of 1x2 parabolic tapered MMI Coupler with a width of 26  $\mu\text{m}$  and waveguide (input/output) of 2 to 6  $\mu\text{m}$  is presented in Figure 4-21, while the simulation of optical field propagation (XZ Slice) is displayed in Figure 4-22.

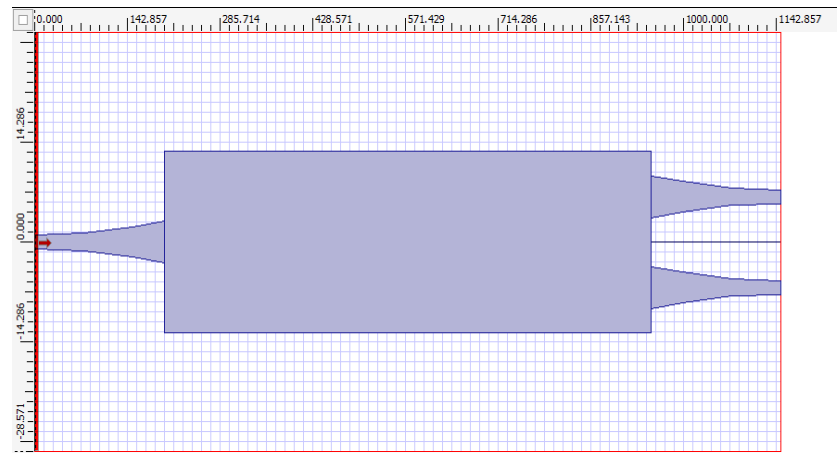


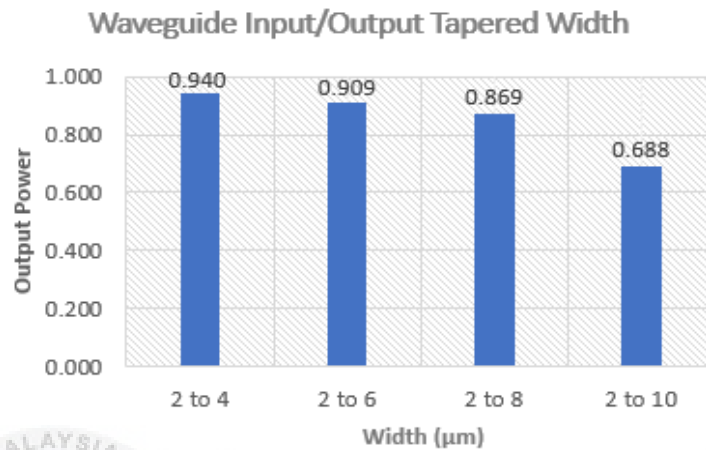
**Figure 4-21: Parabolic tapered 1x2 MMI Coupler structure in OptiBPM Designer, input/output width=2 to 6  $\mu\text{m}$ .**



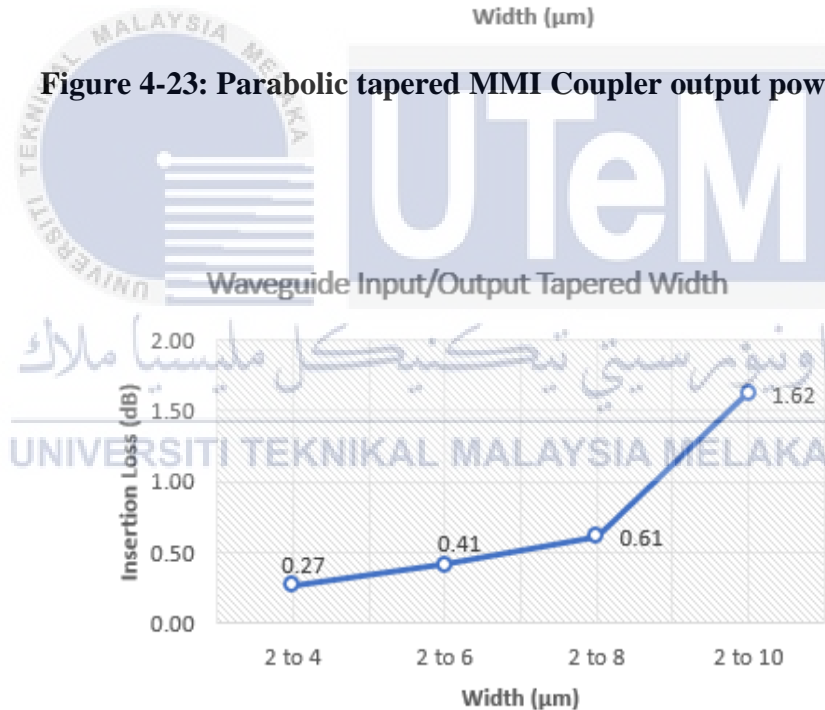
**Figure 4-22: Optical field propagation of parabolic tapered 1x2 MMI Coupler in OptiBPM Analyzer, input/output width=2 to 6  $\mu\text{m}$ .**

Figure 4-23 shows the output power ratio of four (4) different size of input and output waveguide width. The output power is the total power in both output arms. The results indicate that the MMI splitter design width of 2  $\mu\text{m}$  to 4  $\mu\text{m}$  gave the highest splitting ratio and optimal power output. Next, the insertion loss for each design is calculated, as shown in Figure 4-24. Although it was well-known that a wider waveguide gave a stable transmitted power than a narrower waveguide, the tapered

design allows a more guided way for the optical signal to propagate in the MMI region and produce less insertion loss. In summary, the input/output waveguide width depends on the ratio of its width and the MMI region width.



**Figure 4-23: Parabolic tapered MMI Coupler output power ratio.**



**Figure 4-24: Parabolic tapered MMI Coupler insertion loss (IL).**

#### 4.7 Performance Evaluation Between Different Tapered Structure.

Modelling different tapered structures of multimode interference (MMI) and comparing the performance of each design are the two main objectives of this project. After utilizing the beam propagation method (OptiBPM Software), the optimal performance of each design in terms of insertion loss and structure compactness (length and width) are compared and analyzed.

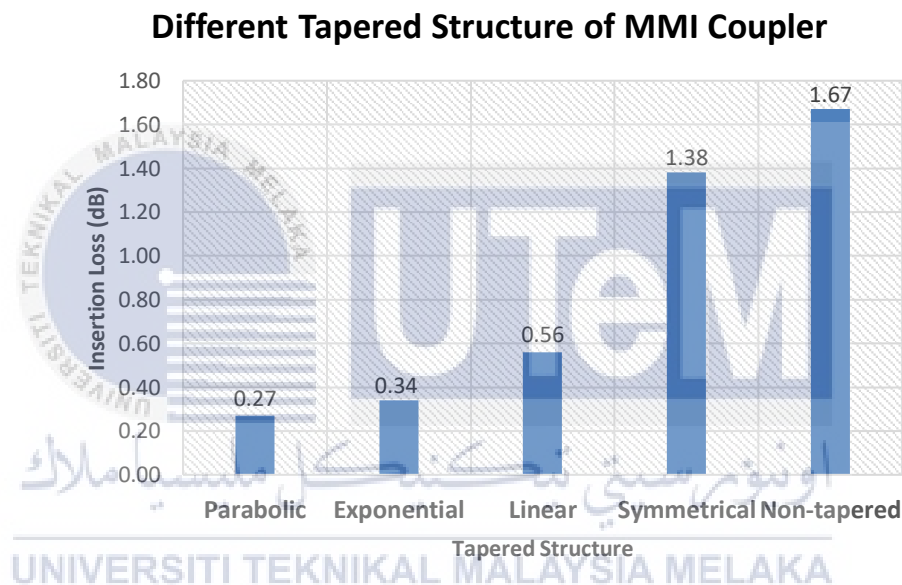


**Figure 4-25: Insertion loss of different tapered MMI Coupler.**

Figure 4-25 displays five (5) MMI couplers with different tapered structures that have been successfully designed and simulated. To obtain optimal performance, two (2) parameters on the MMI coupler structure are precisely calculated and measured. First is the MMI Coupler's length, and second is the position of the output waveguide.

Parabolic tapered with a dimension of 26  $\mu\text{m}$  wide and 750  $\mu\text{m}$  long has produced the lowest insertion loss of 0.27 dB, followed by exponential tapered with 0.34 dB of insertion loss. Whilst linear and symmetrical tapered has an insertion loss of 0.56 and 1.38, respectively. The non-tapered MMI coupler has the worst performance (1.67 dB) compared to the other four tapered designs. Compared to the other structure, the parabolic tapered structure has a tilted waveguide, which allows for improved optical signal splitting. Furthermore, this allows the phase tilt of the optical signal along the coordinate system to the end of the structure. The performance produced by parabolic tapered in this research is in line with studies conducted by previous researchers, such as (Hanim et al., n.d.; Levy, 1998; Wei et al., 2001).

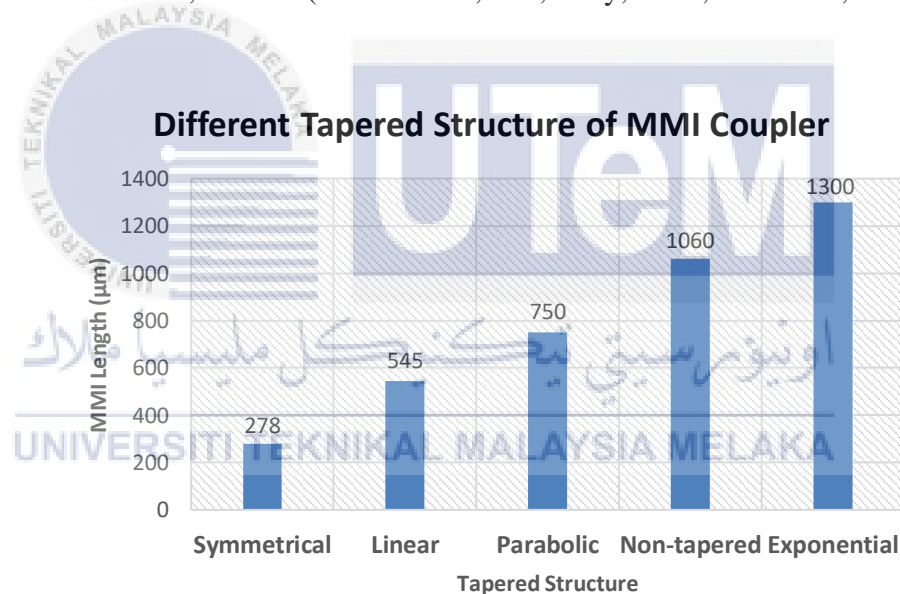


**Figure 4-26: Length of different tapered MMI Coupler.**

Multimode interference (MMI) coupler is a compact and sensitive device. Most of the research focuses on reducing the size of MMI by modifying its structure and, at the same time, maintaining the performance. Figure 4-26 illustrates the length of five (5) different tapered structures of MMI coupler. The symmetrical tapered can be formed at a minimum length of 278  $\mu\text{m}$ . This shows that this structure has the most

compact size compared to the other structures. Although the insertion loss for symmetrical tapered cannot overcome parabolic tapered, symmetrical tapered can be an option if an optical system focuses on a minimal size.

Overall, the performance produced by each model in this research is in line with the studies conducted by previous researchers, as illustrated in Table 4-4.

**Table 4-4: Performance of Different Tapered Structure of MMI Couplers.**

	<b>Tapered</b>	<b>Dimension</b>	<b>Insertion Loss (dB)</b>
Chack et al., 2015	Non	1x2 splitter, W=3.4 $\mu\text{m}$ L=240 $\mu\text{m}$	0.857
<i>This research</i>	Non	1x2 splitter, W=30 $\mu\text{m}$ L=1060 $\mu\text{m}$	1.67
(Halir, Ortega-Moñux, et al., 2009)	Linear	2x2 MMI, W=12.8 $\mu\text{m}$ L=456 $\mu\text{m}$	<1
<i>This research</i>	Linear	1x2 splitter, W= 22 $\mu\text{m}$ L=545 $\mu\text{m}$	0.56
Levy, 1998	Parabolic	4x4 splitter, L = 33 $\mu\text{m}$ W = 20 $\mu\text{m}$	0.8
<i>This research</i>	Parabolic	1x2 splitter, W= 26 $\mu\text{m}$ L=750 $\mu\text{m}$	0.27
(Le et al., 2014)	Exponential	1x2 splitter, L=1391 $\mu\text{m}$ W= 15 $\mu\text{m}$ – 18 $\mu\text{m}$	1.17
<i>This research</i>	Exponential	1x2 splitter, W= 34 $\mu\text{m}$ L=1300 $\mu\text{m}$	0.34

## CHAPTER 5

### CONCLUSION AND FUTURE WORKS



#### 5.1 Conclusion.

All three objectives of this research have been achieved, starting with modelling different tapered structures of MMI couplers, simulating the model in OptiBPM software, and finally analyzing the performance through output power ratio and insertion loss. The concept behind the self-imaging principle was utilized to demonstrate the versatility of MMI coupler. This research studies the effect on MMI performance by varying MMI width, MMI length dan also tapering the input/output waveguide.

The first objective of this research is to model five (5) different tapered structures of MMI coupler. The non-tapered, linear, parabolic, exponential, and

symmetrical tapered are modelled in OptiBPM designer. The dimension of each design is precisely calculated and sketched. The design of 1x2 MMI coupler is created based on five structure widths, 22  $\mu\text{m}$ , 26  $\mu\text{m}$ , 30  $\mu\text{m}$ , 34  $\mu\text{m}$  and 38  $\mu\text{m}$ . At the same time, the length of each design is set depending on the self-imaging principle and its formula.

To fulfil the second objective of this research, the simulation work was implemented using OptiBPM 2D simulation tools, a waveguide optics design software produced by Optiwave System Inc. Among the observations are optical field propagation (XZ slice), refractive index propagation (XZ slice), and cut view.

Finally, the performance of each model is analyzed to fulfil the third objective of this research. The quality and performance of each design are determined based on an output splitting ratio of 0.5, where the equivalent splitting occurs at the couplers output. Measurements of output power splitting ratio were obtained from OptiBPM Analyzer mode. The insertion loss is then calculated based on the measurement result.

Parabolic tapered with a width of 26  $\mu\text{m}$  has produced the lowest insertion loss of 0.27 dB. On the other hand, the non-tapered MMI coupler has the worst performance (1.67 dB) compared to the other four tapered designs. The parabolic tapered structure has a tilted waveguide, which allows for improved optical signal splitting. Furthermore, this allows the phase tilt of the optical signal along the coordinate system to the end of the structure.

The symmetrical tapered is the most compact MMI coupler that can be produced with a minimum length of 278  $\mu\text{m}$ . Although the symmetrical tapered insertion loss is higher than parabolic tapered, it would be a good option for an optical



system that focuses on a compact device. A low insertion loss and size compactness demonstrated in this research have portrayed this device's prospect in photonics applications.

## 5.2 Future Works and Recommendations.

The principle for future technology is optimal power, compact, high speed and cost-effective. Therefore, further research should focus on reducing the size of MMI by modifying its structure and, at the same time, improving the performance. This study was only conducted on 2-dimensional structure.

Further research needs to be conducted in 3-dimensional and subsequently fabricated. Result from simulation and fabrication might be differ. Simulation is in ideal conditions, whereas many external effects/parameters need to be considered in fabrication.

## REFERENCES

- Al-Azzawi, A. (2017). *Fiber optics: Principles and advanced practices*. CRC Press.
- Besse, P. A., Bachmann, M., Melchior, H., Soldano, L. B., & Smit, M. K. (1994). Optical bandwidth and fabrication tolerances of multimode interference couplers. *Journal of Lightwave Technology*, 12(6), 1004–1009.
- Chack, D., Agrawal, N., & Raghuwanshi, S. K. (2014). To analyse the performance of tapered and MMI assisted splitter on the basis of geographical parameters. *Optik*, 125(11), 2568–2571. <https://doi.org/10.1016/j.ijleo.2013.11.019>
- Chack, D., Kumar, V., & Raghuwanshi, S. K. (2015). Design and performance analysis of InP/InGaAsP-MMI based 1310/1550-nm wavelength division demultiplexer with tapered waveguide geometry. *Opto-Electronics Review*, 23(4), 271–277.
- Cherchi, M., Harjanne, M., Ylinen, S., Kapulainen, M., Vehmas, T., Aalto, T., & Technical, V. T. T. (2016). Flat-top MZI filters: A novel robust design based on MMI splitters. *Proceedings of SPIE*, 9752, 1–9. <https://doi.org/10.1117/12.2210937>

Chuang, R. W., Hsu, M.-T., Chang, Y.-C., Lee, Y.-J., & Chou, S.-H. (2012). Integrated multimode interference coupler-based Mach–Zehnder interferometric modulator fabricated on a silicon-on-insulator substrate. *IET Optoelectronics*, 6(3), 147. <https://doi.org/10.1049/iet-opt.2010.0106>

Emara, M. K. (2021). *A Review of Optical Coupler Theory, Techniques, and Applications*.

Fujisawa, T., & Koshiba, M. (2006). Theoretical investigation of ultrasmall polarization-insensitive  $1/\sqrt{2}$  multimode interference waveguides based on sandwiched structures. *IEEE Photonics Technology Letters*, 18(11), 1246–1248.

Halir, R., Ortega-Monux, A., Molina-Fernandez, I., Wangüemert-Perez, J. G., Cheben, P., Dan-Xia Xu, Lamontagne, B., & Janz, S. (2009). Compact High-Performance Multimode Interference Couplers in Silicon-on-Insulator. *IEEE Photonics Technology Letters*, 21(21), 1600–1602. <https://doi.org/10.1109/LPT.2009.2030689>

Halir, R., Ortega-Monux, A., Molina-Fernández, Í., Wangüemert-Pérez, J. G., Cheben, P., Xu, D. X., Lamontagne, B., & Janz, S. (2009). Compact high-performance multimode interference couplers in silicon-on-insulator. *IEEE Photonics Technology Letters*, 21(21), 1600–1602. <https://doi.org/10.1109/LPT.2009.2030689>

Hamamoto, K., Gini, E., Holtmann, C., & Melchior, H. (2001). Single-transverse-mode active multi-mode-interferometer 1.45  $\mu\text{m}$  high power laser diode. *Applied Physics B*, 73(5), 571–574.

Hanim, A. R., Zamil, N. S. M., Hazura, H., Zain, A. S. M., Salehuddin, F., & Idris, S. K. (n.d.). *The performance analysis of different tapered structures of MMI couplers for MZI modulators on Silicon-On- Insulator (SOI)*. 5.

Huang, M. (2003). Stress effects on the performance of optical waveguides. *International Journal of Solids and Structures*, 40(7), 1615–1632.

Izutsu, M., Nakai, Y., & Sueta, T. (1982). Operation mechanism of the single-mode optical-waveguide Y junction. *Optics Letters*, 7(3), 136–138.

Jiang, X., Li, X., Zhou, H., Yang, J., Wang, M., Wu, Y., & Ishikawa, S. (2005). Compact variable optical attenuator based on multimode interference coupler. *IEEE Photonics Technology Letters*, 17(11), 2361–2363.

Ke, X., Wang, M. R., & Li, D. (2006). All-optical controlled variable optical attenuator using photochromic sol gel material. *IEEE Photonics Technology Letters*, 18(9), 1025–1027.

Keiser, G. (2003). Optical fiber communications. *Wiley Encyclopedia of Telecommunications*.

Kogelnik, H., & Schmidt, R. V. (1976). Switched directional couplers with alternating  $\Delta\beta$ . *IEEE Journal of Quantum Electronics*, 12(7), 396–401.

Le, Z., Yin, L., Huang, S., & Fu, M. (2014). The cascaded exponential-tapered multimode interference couplers based triplexer design for FTTH system. *Optik*, 125(16), 4357–4362.

- Levy, D. S. (1998). A New Design for Ultracompact Multimode Interference-Based 2 × 2 Couplers. *IEEE PHOTONICS TECHNOLOGY LETTERS*, 10(1), 3.
- Li, Z., Chen, Z., & Li, B. (2005). Optical pulse controlled all-optical logic gates in SiGe/Si multimode interference. *Optics Express*, 13(3), 1033–1038.
- Liow, T. Y., Ang, K. W., Fang, Q., Song, J. F., Xiong, Y. Z., Yu, M. Bin, Lo, G. Q., & Kwong, D. L. (2010). Silicon modulators and germanium photodetectors on SOI: Monolithic integration, compatibility, and performance optimization. *IEEE Journal on Selected Topics in Quantum Electronics*, 16(1), 307–315. <https://doi.org/10.1109/JSTQE.2009.2028657>
- Liu, A., Jones, R., Liao, L., Samara-Rubio, D., Rubin, D., Cohen, O., Nicolaescu, R., & Paniccia, M. (2004). A high-speed silicon optical modulator based on a metal–oxide– semiconductor capacitor. *Nature Publishing Group*, 427, 615–618. <https://doi.org/10.1038/nature02279.1>
- Marris-Morini, D., Vivien, L., Fédéli, J. M., Cassan, E., Lyan, P., & Laval, S. (2008). Low loss and high speed silicon optical modulator based on a lateral carrier depletion structure. *Optics Express*, 16(1), 334–339. <https://doi.org/10.1364/OE.16.000334>
- Okamoto, K. (2006). *Fundamentals of optical waveguides*. Academic press.
- Pachnicke, S., Roppelt, M., Eiselt, M., Magee, A., Turnbull, P., & Elbers, J.-P. (2012). Investigation of wavelength control methods for next generation passive optical access networks. *European Conference and Exhibition on Optical Communication*, P6-02.

- Quan, Y. jun, Han, P. de, Ran, Q. jiang, Zeng, F. ping, Gao, L. peng, & Zhao, C. hua. (2008). A photonic wire-based directional coupler based on SOI. *Optics Communications*, 281(11), 3105–3110. <https://doi.org/10.1016/j.optcom.2008.02.007>
- Razak, H. A., Haroon, H., Zain, A. S. M., Menon, P. S., Shaari, S., & Mukhtar, W. M. (2015). On the performance of Mach-Zehnder-Interferometer (MZI) optical modulator on silicon-on-insulator (SOI). *2015 IEEE Regional Symposium on Micro and Nanoelectronics (RSM)*, 1–4. <https://doi.org/10.1109/RSM.2015.7355026>
- Sahu, P. P. (2011). Double S-bend structure for a compact two mode interference coupler. *Applied Optics*, 50(3), 242–245.
- Sahu, P. P. (2013). An Ultra Compact multi Mode Interference Coupler with Parabolic Down Tapered Geometry. *Procedia Engineering*, 64, 215–223. <https://doi.org/10.1016/j.proeng.2013.09.093>
- Saleh, B. E., & Teich, M. C. (2019). *Fundamentals of photonics*. John Wiley & sons.
- Samoi, E., Benezra, Y., & Malka, D. (2020). An ultracompact 3×1 MMI power-combiner based on Si slot-waveguide structures. *Photonics and Nanostructures - Fundamentals and Applications*, 39, 100780. <https://doi.org/10.1016/j.photonics.2020.100780>
- Shaim, M. H. A., & Khan, M. R. H. (2011). Design and simulation of a low loss optical fiber coupler. *International Journal of Electronics and Communication Engineering*, 4(5), 473–482.

Shi, Y., Anand, S., & He, S. (2007). A polarization-insensitive 1310/1550-nm demultiplexer based on sandwiched multimode interference waveguides. *IEEE Photonics Technology Letters*, *19*(22), 1789–1791.

Shi, Y., Dai, D., & He, S. (2005). Improved performance of a silicon-on-insulator-based multimode interference coupler by using taper structures. *Optics Communications*, *253*(4–6), 276–282.

Soldano, L. B., & Pennings, E. C. M. (1995). Optical multi-mode interference devices based on self-imaging: Principles and applications. *Journal of Lightwave Technology*, *13*(4), 615–627. <https://doi.org/10.1109/50.372474>

Thomson, D. J., Hu, Y., Reed, G. T., & Fedeli, J.-M. (2010). Low Loss MMI Couplers for High Performance MZI Modulators. *IEEE Photonics Technology Letters*, *22*(20), 1485–1487. <https://doi.org/10.1109/LPT.2010.2063018>

Wang, F., Yang, J., Chen, L., Jiang, X., & Wang, M. (2006). Optical switch based on multimode interference coupler. *IEEE Photonics Technology Letters*, *18*(2), 421–423.

Wei, H., Yu, J., Zhang, X., & Liu, Z. (2001). Compact 3-dB tapered multimode interference coupler in silicon-on-insulator. *Optics Letters*, *26*(12), 878–880.

Wu, B., Sun, C., Yu, Y., & Zhang, X. (2019). Integrated optical coupler with an arbitrary splitting ratio based on a mode converter. *IEEE Photonics Technology Letters*, *32*(1), 15–18.

Wu, J.-J. (2008). A multimode interference coupler with exponentially tapered waveguide. *Progress In Electromagnetics Research*, *1*, 113–122.

## APPENDIX A

(a) **Project Planning Gantt Chart of PSM 1.**

Project Activities	Week														
	1	2	3	4	5	6	7	8	9	10	11	12	13	14	15
<b>Project Title &amp; Proposal</b>															
Search for Project Title															
Preliminary research and data gathering.															
Proposal defence and presentation.															
<b>Planning &amp; Research Analysis</b>															
Research and data gathering for non-tapered and linear tapered.															
OptiBPM software installation and design tutorial.															
Determine the design specification and outline.															
Non-tapered and linear tapered MMI design.															
Report writing - Chapter 1															
<b>Conceptual Design</b>															
Research for parabolic and exponential tapered.															
Parabolic tapered design.															
Exponential tapered design.															
Tapered MMI region design.															
Report writing - Chapter 2															
<b>Project Report</b>															
Project logbook															
Report writing - Chapter 3															
PSM1 draft report submission.															
Finalization of report and seminar content preparation.															
PSM1 project report submission															
<b>PSM 1 Seminar</b>															





## APPENDIX B

### (a) Performance of Different Tapered Structure of MMI Coupler.

	Dimension	Insertion Loss (dB)	Extinction Ratio (dB)	Modulation Efficiency	E-Field intensity (%)	Other
<b>Non-Tapered</b>						
Sahu, 2013	2x2 MMI L=37 $\mu\text{m}$ W=2w+h	Power contributes to cross output access waveguide.				0.835
Chack et al., 2014	L=650 $\mu\text{m}$	n/a	n/a	n/a	59	n/a
Chack et al., 2015	1x2 splitter W=3.4 $\mu\text{m}$ L=240 $\mu\text{m}$	0.857	11.288	n/a	n/a	n/a
(Hanim et al., n.d.)	W = 38 $\mu\text{m}$ L = 4859 $\mu\text{m}$	5.728	26.0795	0.0571	n/a	n/a
<b>Linear Tapered</b>						
Shi et al., 2005	W = 60 $\mu\text{m}$ L = 2089 $\mu\text{m}$	0.076	n/a	n/a	n/a	0.068 of non-uniformity
(Halir, Ortega-Moñux, et al., 2009)	2x2 MMI W=12.8 $\mu\text{m}$ L=456 $\mu\text{m}$	<1	>22	n/a	n/a	n/a
Thomson et al, 2010	1x2 splitter W = 6 $\mu\text{m}$ L = 32 $\mu\text{m}$	n/a	> 32	n/a	n/a	n/a
Domenech, 2014	2x2 MMI Coupler L= 257.6 $\mu\text{m}$ W = 10 $\mu\text{m}$	n/a	n/a	n/a	n/a	0.6 dB Excess loss
Chack et al., 2014	L=650 $\mu\text{m}$	n/a	n/a	n/a	73	n/a
Chack et al., 2015	1x2 splitter W=3.4 $\mu\text{m}$ L=240 $\mu\text{m}$	0.255	19.487	n/a	n/a	n/a
Tian et al. 2015	4x4 MMI L= 182.6 $\mu\text{m}$ W = 10.2 $\mu\text{m}$	5.6	n/a	n/a	n/a	n/a
(Cherchi et al., 2016)	W = 350 $\mu\text{m}$ L = 2 mm	<1.5	>15	n/a	n/a	n/a
(Hanim et al., n.d.)	1x2 splitter W = 38 $\mu\text{m}$ L = 4859 $\mu\text{m}$	5.725	28.4298	0.0565	n/a	n/a

	Dimension	Insertion Loss (dB)	Extinction Ratio (dB)	Modulation Efficiency	E-Field intensity (%)	Other
<b>Parabolic Tapered</b>						
Levy, 1998	4x4 power splitter L = 33 $\mu$ m W <sub>o</sub> = 20 $\mu$ m	0.8	n/a	n/a	n/a	n/a
Wei et al., 2001	1x2 splitter L = 398 $\mu$ m	n/a	n/a	n/a	n/a	0.28 of uniformity & 9.9 dB excess loss
Sahu, 2013	2x2 MMI L=37 $\mu$ m W=2w+h	Power contributes to cross output access waveguide.				0.988
(Hanim et al., n.d.)	1x2 splitter W = 38 $\mu$ m L = 4859 $\mu$ m	4.592	33.3305	0.0572	n/a	n/a
<b>Exponential Tapered</b>						
J.-J. Wu, 2008	1x2 splitter W <sub>o</sub> = 24 $\mu$ m	Sum of output power of exponential tapered larger than parabolic and with shorter length.				
(Le et al., 2014)	1x2 splitter L = 1391 $\mu$ m W= 15 $\mu$ m – 18 $\mu$ m	1.17dB	n/a	n/a	n/a	n/a

اوتور سیتی تکنیکل ملیسیا ملاک

UNIVERSITI TEKNIKAL MALAYSIA MELAKA